

MODEL-FREE WIND FARM POWER  
PRODUCTION OPTIMIZATION USING  
MULTI-RESOLUTION OPTIMIZED  
RELATIVE STEP SIZE RANDOM SEARCH

MOK REN HAO

UMP

Master of Science

UNIVERSITI MALAYSIA PAHANG

## UNIVERSITI MALAYSIA PAHANG

### DECLARATION OF THESIS AND COPYRIGHT

Author's Full Name : MOK REN HAO

Date of Birth : 14 SEPTEMBER 1991

Title : MODEL-FREE WIND FARM POWER PRODUCTION  
OPTIMIZATION USING MULTI-RESOLUTION  
OPTIMIZE RELATIVE STEP SIZE RANDOM SEARCH

Academic Session : Sem 2 2018/2019

I declare that this thesis is classified as:

- CONFIDENTIAL (Contains confidential information under the Official Secret Act 1997)\*
- RESTRICTED (Contains restricted information as specified by the organization where research was done)\*
- OPEN ACCESS I agree that my thesis to be published as real-time open access (Full Text)

I acknowledge that Universiti Malaysia Pahang reserves the following rights:

1. The Thesis is the Property of Universiti Malaysia Pahang
2. The Library of Universiti Malaysia Pahang has the right to make copies of the thesis for the purpose of research only.
3. The Library has the right to make copies of the thesis for academic exchange.

Certified by:

\_\_\_\_\_  
(Student's Signature)

910914-03-5027  
New IC/Passport Number  
Date: 1 APRIL 2019

\_\_\_\_\_  
(Supervisor's Signature)

MOHD ASHRAF BIN AHMAD  
Name of Supervisor  
Date: 1 APRIL 2019

NOTE : \* If the thesis is CONFIDENTIAL or RESTRICTED, please attach a thesis declaration letter.

### **SUPERVISOR'S DECLARATION**

I hereby declare that I have checked this thesis and in my opinion, this thesis is adequate in terms of scope and quality for the award of the degree of Master of Science.

---

(Supervisor's Signature)

Full Name : DR. MOHD ASHRAF BIN AHMAD

Position : SENIOR LECTURER

Date : 1 APRIL 2019



UMP

### **STUDENT'S DECLARATION**

I hereby declare that the work in this thesis is based on my original work except for quotations and citations which have been duly acknowledged. I also declare that it has not been previously or concurrently submitted for any other degree at Universiti Malaysia Pahang or any other institutions.

---

(Student's Signature)

Full Name : MOK REN HAO

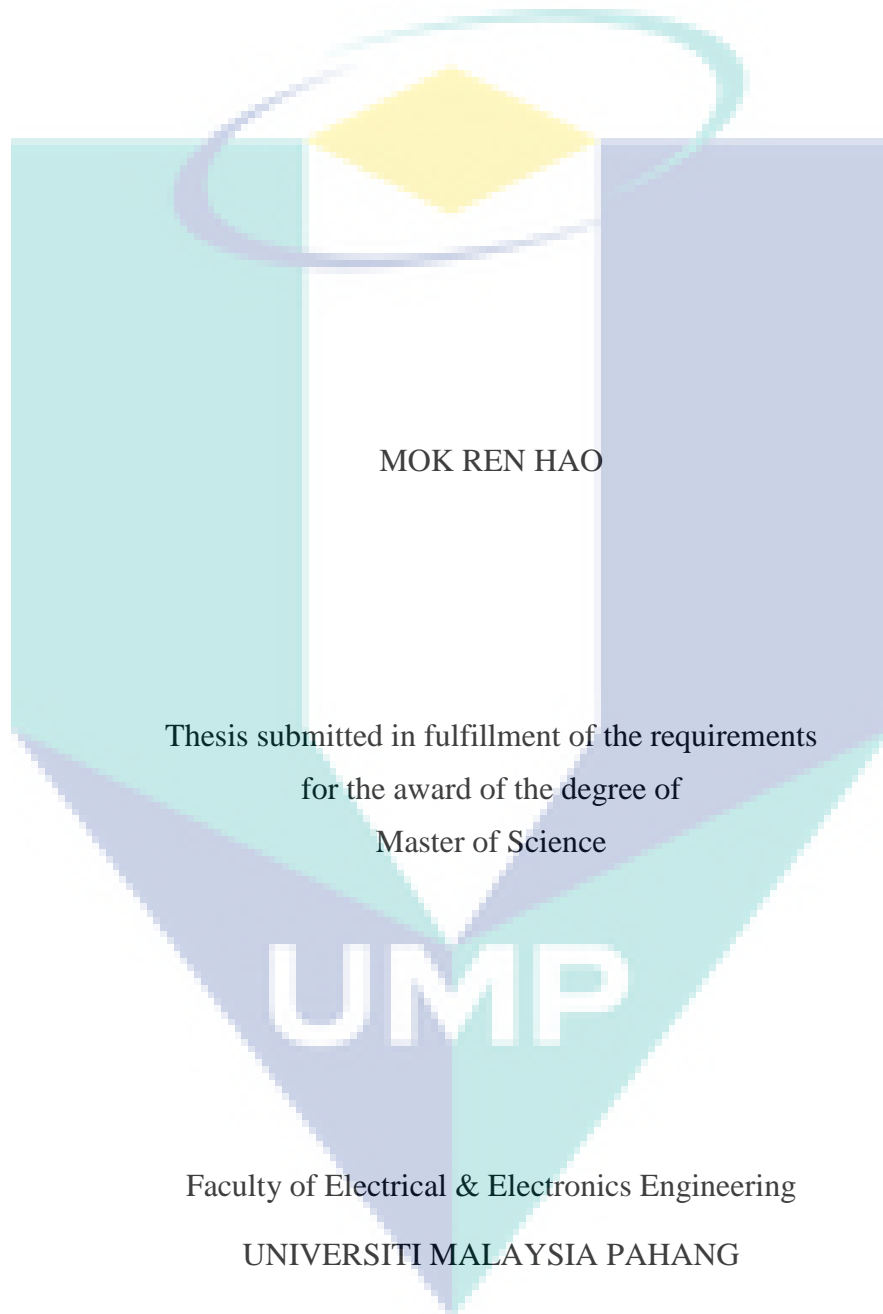
ID Number : MEL16011

Date : 1 APRIL 2019



UMP

Model-Free Wind Farm Power Production Optimization Using  
Multi-Resolution Optimized Relative Step Size Random Search



MOK REN HAO

Thesis submitted in fulfillment of the requirements  
for the award of the degree of  
Master of Science

UMP

Faculty of Electrical & Electronics Engineering

UNIVERSITI MALAYSIA PAHANG

APRIL 2019

## ACKNOWLEDGEMENTS

Firstly, I would like to thank my supervisor, Dr. Mohd Ashraf Bin Ahmad for being particularly supportive during the pursue of my Master's Degree in University Malaysia Pahang (UMP). His excellent academic guidance and vast knowledge had been valuable in assisting me towards the completion of my research. His patience in ensuring the fruitful progress of my study is highly valued, and the time he spent doing so was beyond the call of duty.

I would also like to acknowledge my most profound appreciation for the tremendous support given to me by my family, especially my mother. They had given both spiritual and emotional encouragement, as well as financial assistance in helping me towards fulfilling my dream. My beloved mother was the shoulder to lean on, especially when I was faced with challenges as my study progressed during these two years of research. I would also like to thank my colleagues for the friendship and supportive words they had given me.

Finally, I would like to take this opportunity to thank the Institute of Postgraduate Study (IPS) of UMP for providing me with two years of financial assistance from the Master Research Scheme (MRS). In addition to that, I had received financial support for publications from the Post-Graduate Research Scheme (PGRS1703105). These aids had given me considerable amount of financial relief, which further helped me tremendously in the successful completion of my study.



UMP

## ABSTRAK

Kajian ini menyelidiki prestasi kaedah *Multi-Resolution Optimize Relative Step Size Random Search* (MR-ORSSRS) untuk meningkatkan jumlah pengeluaran tenaga ladang angin. Penyelidikan ini telah dilakukan mengikut susunan ladang angin *Horns Rev* yang mempunyai 80 turbin angin untuk mengatasi masalah seperti perbezaan arah angin antara  $170^\circ$ ,  $200^\circ$ ,  $220^\circ$ ,  $240^\circ$ ,  $250^\circ$  dan  $270^\circ$ , lima turbin angin yang mengalami kerosakan serta perubahan angin yang tidak tertentu. Pengenaan fungsi *Multi-Resolution* daripada (Ahmad *et al.*, 2014) adalah digunakan untuk menambahbaik kadar penumpuan *Optimize Relative Step Size Random Search* demi meningkatkan jumlah pengeluaran tenaga ladang angin secara langsung. Fungsi *Multi-Resolution* (MR) ini boleh meningkatkan kelajuan kadar penumpuan dengan ketara kerana kaedah ini mengusahakan parameter kawalan berdimensi dengan beberapa tahap penambahbaikan. Secara khususnya, fungsi ini memulakan penambahbaikan dengan parameter kawalan dimensi rendah dan meningkatkan jumlah dimensi pada tahap penambahbaikan seterusnya. Oleh itu, usaha pengiraan untuk mendapatkan parameter kawalan optimum boleh dikurangkan. Walaupun MR-SPSA dikenalkan untuk menyelesaikan masalah berdimensi tinggi secara langsung dengan kadar penumpuan yang laju, ia tidak mampu menghasilkan jumlah tenaga ladang angin yang optimum. Ini disebabkan, SPSA merupakan kaedah penambahbaikan yang tidak mempunyai daya ingatan oleh itu, ia tidak berupaya untuk menyimpan parameter kawalan optimum yang dihasilkan. Di samping itu, ORSSRS adalah kaedah penambahbaikan yang mempunyai daya ingatan. Justeru, ia bermampu untuk menyimpan parameter kawalan optimum sementara menghasilkan penambahbaikan yang stabil. Namun demikian, kaedah ORSSRS sendiri tidak mampu membekalkan kadar penumpuan yang mencukupi untuk menyelesaikan masalah ladang angin secara langsung. Oleh itu, fungsi MR digabungkan demi meningkatkan kadar penumpuan kaedah ORSSRS. Dalam kajian ini, prestasi kaedah MR-ORSSRS dibandingkan dengan kaedah MR-SPSA dari segi kadar penumpuan, ketepatan dan kekukuhan dalam peningkatan jumlah pengeluaran tenaga ladang angin. Hasilnya menunjukkan kaedah MR-ORSSRS telah menewaskan kaedah penanda aras MR-SPSA dari segi kadar penumpuan bagi semua kes kajian. Khususnya, ia telah menambahbaik kadar penumpuan untuk kes perbezaan arah angin antara  $170^\circ$ ,  $200^\circ$ ,  $220^\circ$ ,  $240^\circ$ ,  $250^\circ$  dan  $270^\circ$  sebanyak 88.89%, 88.89%, 41.66%, 88.89%, 88.89% dan 66.67% . Sementara itu, 66.67% untuk kes lima turbin angin yang mengalami kerosakan. Selain itu, kaedah MR-ORSSRS telah berjaya meningkatkan jumlah pengeluaran tenaga ladang angin dalam mengatasi masalah perbezaan arah angin antara  $170^\circ$ ,  $200^\circ$ ,  $220^\circ$ ,  $240^\circ$  dan  $270^\circ$  serta kegagalan turbin angin berbanding kaedah MR-SPSA. Dari segi kadar penumpuan, MR-ORSSRS juga menghasilkan kadar penumpuan yang lebih laju dalam mengatasi masalah perbezaan arah angin sementara kegagalan turbin angin melanda. Oleh demikian, ini telah menunjukkan kaedah MR-ORSSRS yang dicadangkan adalah berkesan untuk menghasilkan jumlah pengeluaran tenaga dengan kadar penumpuan yang lebih laju walaupun berlaku kes kegagalan turbin angin dan perubahan angin yang tidak tertentu berbanding dengan kaedah penanda aras MR-SPSA.

## ABSTRACT

This study investigates the performance of Multi-Resolution Optimize Relative Step Size Random Search (MR-ORSSRS) based method in maximizing the total power production of wind farms. The performance is investigated based on the Horns Rev wind farm layout which consists of 80 wind turbines under the case studies of different wind directions at  $170^\circ$ ,  $200^\circ$ ,  $220^\circ$ ,  $240^\circ$ ,  $250^\circ$  and  $270^\circ$ , five wind turbines failures and non-static wind variations. The implementation of Multi-Resolution (MR) function is used to improve the convergence speed of the Optimize Relative Step Size Random Search in the case of maximizing the total power production of a wind farm in real-time optimization. The MR function is significant in improving the convergence speed since this approach exploits the dimension of the design parameter using several optimization stages. In particular, it firstly adopts a small size of design parameter tuning followed by a bigger size of design parameter tuning in the following stages. Therefore, it is expected that less computation effort is required to obtain the optimal design parameter. Even though the Multi-Resolution Stochastic Perturbation Simultaneous Approximation (MR-SPSA) is developed to solve the real-time high-dimensional problem with faster convergence, the obtained total power production of the wind farm is still not optimum. This is because the SPSA is a memory-less structure type optimization that limits the storage of the best design parameter. Alternatively, ORSSRS based method is a memory type optimization structure. Hence, it can store the best design parameter value while producing consistent objective function. However, the ORSSRS based method alone does not have the sufficient convergence speed to optimize wind farm problem in real time. Therefore, the MR function is implemented to improve the convergence speed of the ORSSRS based method. In this study, the performance of MR-ORSSRS based method is compared with MR-SPSA based method in terms of the convergence speed, accuracy, and robustness in maximizing the total power production of Horns Rev wind farm. The results show that MR-ORSSRS based method outperforms the benchmark MR-SPSA based method in terms of the convergence speed of all the study cases. In particular, it can improve the convergence speed of incoming wind direction at  $170^\circ$ ,  $200^\circ$ ,  $220^\circ$ ,  $240^\circ$ ,  $250^\circ$  and  $270^\circ$  by 88.89%, 88.89%, 41.66%, 88.89%, 88.89% and 66.67%, respectively. However, in the case of the five wind turbine failures, the speed of the incoming wind direction is 66.67%. Moreover, the MR-ORSSRS based method produces better total power production for wind direction at  $170^\circ$ ,  $200^\circ$ ,  $220^\circ$ ,  $240^\circ$  and  $270^\circ$ , as well as wind turbines failures compared to the MR-SPSA based method. In term of the convergence speed, the MR-ORSSRS based method produces higher convergence speed for all the wind direction cases even in the wind turbines failure cases. Hence, it is proven that the proposed MR-ORSSRS based method is effective in producing better total power production with faster convergence speed even with turbines failure and time-varying wind compared to the benchmark MR-SPSA based method.



## TABLE OF CONTENT

<b>DECLARATION</b>	
<b>TITLE PAGE</b>	
<b>ACKNOWLEDGEMENTS</b>	<b>ii</b>
<b>ABSTRAK</b>	<b>iii</b>
<b>ABSTRACT</b>	<b>iv</b>
<b>TABLE OF CONTENT</b>	<b>v</b>
<b>LIST OF TABLES</b>	<b>viii</b>
<b>LIST OF FIGURES</b>	<b>ix</b>
<b>LIST OF SYMBOLS</b>	<b>xi</b>
<b>LIST OF ABBREVIATIONS</b>	<b>xiii</b>
<b>CHAPTER 1 INTRODUCTION</b>	<b>1</b>
1.1 Background of Research	1
1.1.1 Micro-siting Optimization of Wind Farm	3
1.1.2 Axial Induction Factor (Controller) Optimization of Wind Farm	4
1.2 Motivation and Problem Statement	5
1.3 Objectives	6
1.4 Scope and Limitations	7
1.5 Overview of the Thesis	7
<b>CHAPTER 2 LITERATURE REVIEW</b>	<b>9</b>
2.1 Introduction	9
2.2 Micro-siting Optimization	10

2.2.1	Software-based Optimization	10
2.2.2	Optimization Algorithms	12
2.2.3	Limitation of Wind Farm Micro-Siting Optimization	13
2.3	Model-based Controller Optimization	13
2.3.1	Doubly Fed Induction Generation (DFIG)	14
2.3.2	Hierarchical wind farm control (HWFC)	14
2.3.3	Distributed Controller	15
2.3.4	Limitation of Model-based Approaches	16
2.4	Model-free Controller Optimization	16
2.4.1	Game Theoretic (GT)	17
2.4.2	Maximum Power Point Tracking (MPPT)	18
2.4.3	Simultaneous Perturbation Stochastic Approximation (SPSA)	18
2.4.4	Bayesian Ascent (BA)	19
2.4.5	Spiral Dynamic Algorithm (SDA)	20
2.4.6	Extremum-Seeking Control (ESC)	20
2.4.7	Random Search (RS)	21
2.4.8	Optimize Relative Step Size Random Search (ORSSRS)	21
2.5	Summary	22
<b>CHAPTER 3 METHODOLOGY</b>		<b>25</b>
3.1	Introduction	25
3.2	Wind Farm System	26
3.3	Problem Formulation	29
3.4	Random Search Based Optimization Methods	30
3.4.1	Optimized Relative Step Size Random Search	30
3.4.2	Multi-Resolution Optimize Relative Step Size Random Search	33

3.5	Model-free Design for Wind Farm Total Power Production Maximization	36
3.6	Summary	39
<b>CHAPTER 4 RESULTS AND DISCUSSION</b>		<b>41</b>
4.1	Introduction	41
4.2	Horns Rev Wind Farm	42
4.3	The Performance of methods with Different Wind Direction	44
4.4	Performance of Methods with Wind Turbine Failure	53
4.5	Performance of methods with non-static Wind Variation	55
4.6	Summary	57
<b>CHAPTER 5 CONCLUSION</b>		<b>58</b>
5.1	Introduction	58
5.2	Contribution	59
5.3	Recommendations and Future Works	60
<b>REFERENCES</b>		<b>62</b>
<b>LIST OF PUBLICATION</b>		<b>66</b>



UMP

## LIST OF TABLES

Table 3.1	The required convergence time for different sizes of dimension	32
Table 3.2	The required convergence time for different number of wind turbines	32
Table 3.3	Group strategy with the corresponded resolution, $j$	38
Table 4.1	Wind farm parameters	43
Table 4.2	Time interval $T_\omega$ for wake to travel throughout wind farm	44
Table 4.3	Parameters for Algorithm 3.1 (ORSSRS) for wind direction at $170^\circ$	45
Table 4.4	Parameters for Algorithm 3.3 (MR-ORSSRS)	45
Table 4.5	Group number of the second resolution $G(2)$ for Algorithm 3.3 (MR-ORSSRS)	47
Table 4.6	Performance analysis of the total power production ( $MW$ ) for MR-ORSSRS, MR-SPSA and ORSSRS with different wind directions. Std.: Standard deviation	51
Table 4.7	Performance analysis of the convergence time (h) for MR-ORSSRS, MR-SPSA and ORSSRS with different wind directions	52
Table 4.8	Performance evaluation of the MR-ORSSRS, MR-SPSA and ORSSRS-based methods with five wind turbine failures	55



UMPA

## LIST OF FIGURES

Figure 1.1	Annual global capacity of the newly installed wind farm from the year 2001 to the year 2017	1
Figure 1.2	Annual global total capacity of installed wind farm from year 2001 to year 2017	2
Figure 1.3	Wake interaction among wind turbines in wind farm	3
Figure 1.4	Analysis of wake effect between wind turbines in wind farm	3
Figure 1.5	The indication of wind speed and direction occurrence frequency known as a wind rose	4
Figure 1.6	Generic optimization block diagram of model-free approach	5
Figure 2.1	Summarized reviews of related literature of this study	9
Figure 2.2	GUI of Wind Farmer 4.2 wind farm micro-siting optimization software with the illustration of wind farm layout and the appearance of with turbines arrangement	11
Figure 2.3	GUI of Wind Farmer 4.2 with the illustration of wind speed and direction according to the wind data acquired from wind rose model	12
Figure 2.4	An example of model-free optimization approach based on the information of input and output	17
Figure 3.1	The expansion of wake in Park model	26
Figure 3.2	Classification of wake effect in Park model by estimating velocity profile of single turbine	27
Figure 3.3	Model-free approach optimization of MR-ORSSRS based method	28
Figure 3.4	Illustration of wake aerodynamic interaction between wind turbines in wind farm	29
Figure 3.5	The illustration of MR-ORSSRS with three resolution step, $m = 3$ and the grey colored crosses are the design parameters, $\vartheta \in \mathbb{R}^9$	34
Figure 3.6	Wind farm consists 9 wind turbines wind direction at $270^\circ$	37
Figure 3.7	Wind farm layout of 16 wind turbines with incoming wind occurring at $225^\circ$ direction	39
Figure 4.1	Horns Rev wind farm layout with incoming wind direction indicator	42
Figure 4.2	The number of wind turbines for the wake to travel through when the wind direction is at $220^\circ$	43
Figure 4.3	The number of wind turbine for the wake to travel through when wind direction occurs at $240^\circ$	44
Figure 4.4	Group selection in the first resolution for the wind direction of $170^\circ$	46
Figure 4.5	Group selection in the second resolution for the wind direction of $170^\circ$	46

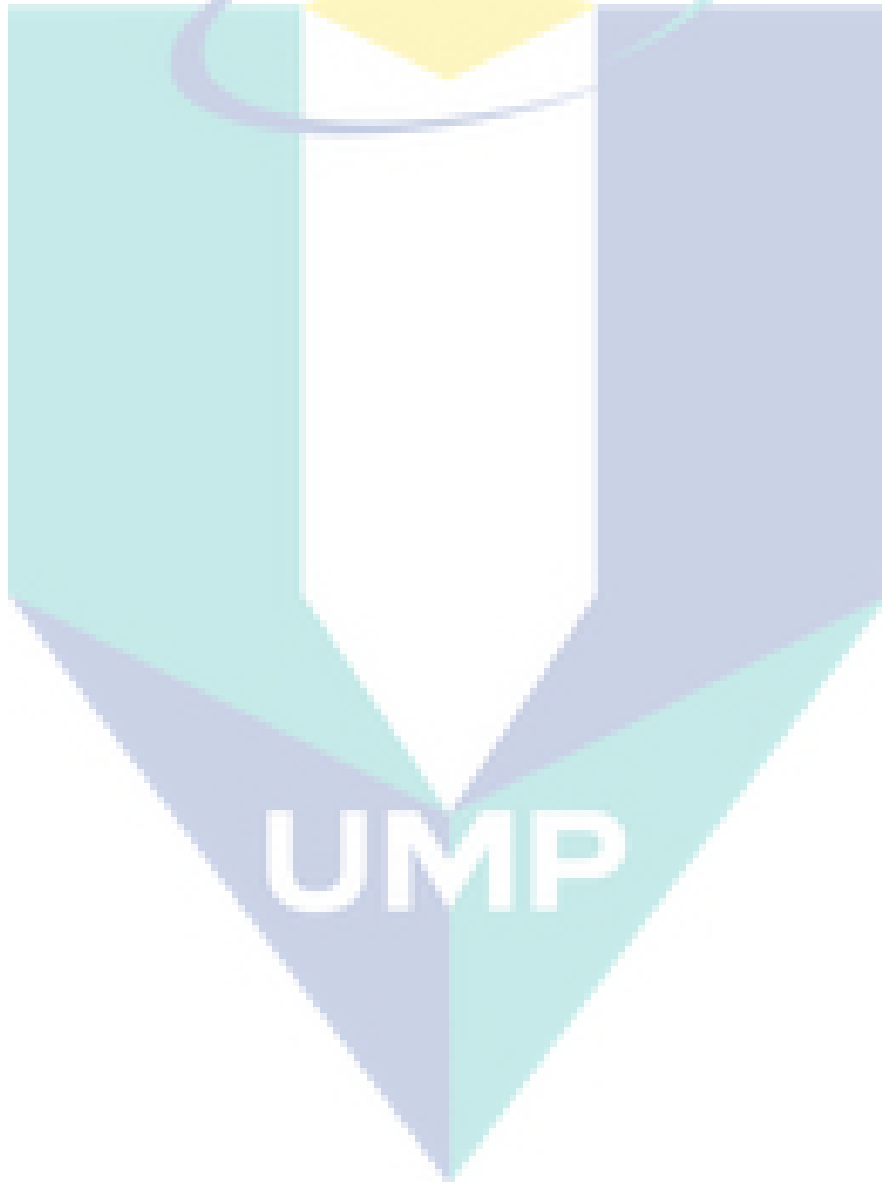
Figure 4.6	Group selection in the first resolution for the wind direction of 200°	47
Figure 4.7	Group selection in the second resolution for the wind direction of 200°	47
Figure 4.8	Results of the total power production $Q(\alpha_1, \alpha_2, \dots, \alpha_{80})$ during the first 10 hours of simulation time when wind occurs at the 170° direction	48
Figure 4.9	Results of the total power production $Q(\alpha_1, \alpha_2, \dots, \alpha_{80})$ in the first 10 hours of simulation time when wind occurs at the 200° direction	48
Figure 4.10	Results of full simulation time of total power production $Q(\alpha_1, \alpha_2, \dots, \alpha_{80})$ when wind is occurring at 170° direction	49
Figure 4.11	Results of the total power production $Q(\alpha_1, \alpha_2, \dots, \alpha_{80})$ during the full simulation time when the wind occurs at the 200° direction	50
Figure 4.12	Horns Rev wind farm layout with five wind turbine failures	53
Figure 4.13	Results of the total power production $Q(\alpha_1, \alpha_2, \dots, \alpha_{80})$ during the first 10 hours of simulation time with failure in five wind turbines	54
Figure 4.14	Results of the total power production $Q(\alpha_1, \alpha_2, \dots, \alpha_{80})$ of 700 hours of simulation time with failure in five wind turbines	54
Figure 4.15	Non-Static incoming wind speed variations of 10 hours simulation time	55
Figure 4.16	Non-Static incoming wind direction variations during 10 hours of simulation time	56
Figure 4.17	Total power improvements of the MR-ORSSRS, MR-SPSA and ORSSRS based methods under non-static incoming wind speed and direction during 10 hours of simulation time	56

UMP

## LIST OF SYMBOLS

$A$	Rotor swept area of the wind turbine
$A^{ov}$	Overlapped rotor swept area of the wind turbine
$D$	Rotor diameter of wind turbine
$e$	Exponential gain
$F$	Objective function
$F^*$	Optimum objective function
$G$	Group of wind turbines
$i$	The number subjected to wind turbine
$j$	Number of resolution
$m$	Maximum number of resolution
$n$	Total number of wind turbine in wind farm
$N$	Total number of designed parameter
$Q$	Power production of wind turbine
$\bar{Q}$	Total power production of wind farm
$r$	Distance to centreline of wind turbine rotor axis
$R$	$n$ -dimensional random vector
$S$	Step size constant
$t$	Number of iteration
$t_{max}$	Termination criterion of ORSSRS
$T_{\omega}$	Time interval for wake to travel throughout wind farm
$V_{\omega}$	Incoming wind speed
$\Delta\bar{V}$	Differences of aggregated wind velocity
$x$	Distance to rotor disk plane of wind turbine
$X$	A set of $n$ wind turbines in wind farm
$\alpha$	Axial induction factor
$\beta$	Update sequence
$\delta$	Negative constant
$\varepsilon$	Termination criterion of MR-ORSSRS
$\gamma$	Objective function of resolution
$\lambda$	A set of wind turbine
$\varphi$	Grouped design parameter of $\vartheta$

$\varphi^*$	Grouped optimal design parameter of $\vartheta^*$
$\emptyset$	Roughness coefficient
$\rho$	Air density
$\mathbb{R}$	Real number
$\vartheta$	Designed parameter
$\vartheta^*$	Optimum design parameter
$\tau$	Time interval for wake to travel to the next wind turbine





## LIST OF ABBREVIATIONS

ASSRS	Adaptive Step Size Random Search
BA	Bayesian Ascent
BO	Bayesian Optimization
COE	Cost of energy
DFIG	Doubly Fed Induction Generation
ESC	Extremum-Seeking Control
FS-MPPT	Fixed Step Maximum Power Point Tracking
FSSRS	Fixed Step Size Random Search
GD-MPPT	Gradient-Descent Maximum Power Point Tracking
GT	Game Theoretic
GUI	Graphical user interface
HWFC	Hierarchical wind farm control
IESC	Individual Extremum-Seeking Control
LQR	Linear-quadratic regulator
MAOA	Multi-agent optimization algorithm
MPPT	Maximum Power Point Tracking
MR-ORSSRS	Multi-Resolution Optimize Relative Step Size Random Search
MR-SPSA	Multi-Resolution Stochastic Perturbation Simultaneous Approximation
NESC	Nest Extremum-Seeking Control
ORSSRS	Optimize Relative Step Size Random Search
PDLPO	Payoff-based distributed learning for Pareto optimality
PSO	Particle Swarm Optimization
ROI	Return of investment
RS	Random Search
SAOA	Single-agent optimization algorithm
SDA	Spiral Dynamic Algorithm
SED	Safe experimental dynamics
SPSA	Stochastic Perturbation Simultaneous Approximation
SRS	Sequential Random Search

## CHAPTER 1

### INTRODUCTION

#### 1.1 Background of Research

Wind energy is one of the most popular sustainable energy. The number of wind farm is increasing rapidly, especially in countries with large, flat landscape such as China, Australia and Denmark. As shown in Figure 1.1 by GWEC (2017), the number of new wind farm installed globally between the year 2001 and 2017 had experienced tremendous fluctuations, skewing towards an increasing trend. The most significant progress had been recorded in the year 2015, where more than 63 MW had been installed, bringing the total wind farm capacity to 432 MW globally. This growth continued in the following years with more than 52 MW being installed for both the year of 2016 and 2017 independently. Further illustrated in Figure 1.2, the total wind farm capacity was accumulated to 539 MW globally at the end of 2017, demonstrating the heightened intensity of wind farm development in recent years. However, many unresolved challenges and rooms for improvement remain to be studied, towards the expansion of wind farm usage and development. Thus, this has prevailed to be a significant research topic, especially within the control research community.

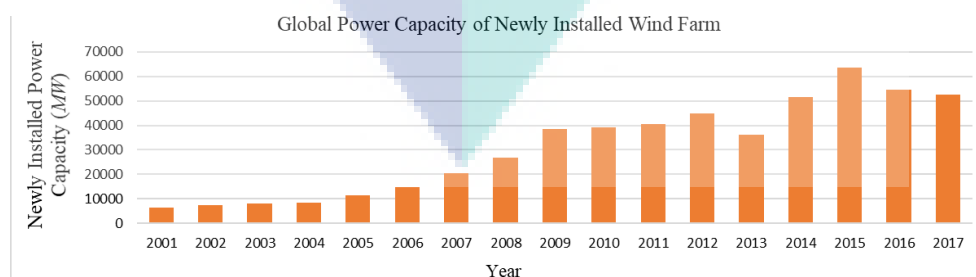


Figure 1.1 Annual global capacity of the newly installed wind farm from the year 2001 to the year 2017

Source: GWEC (2017)

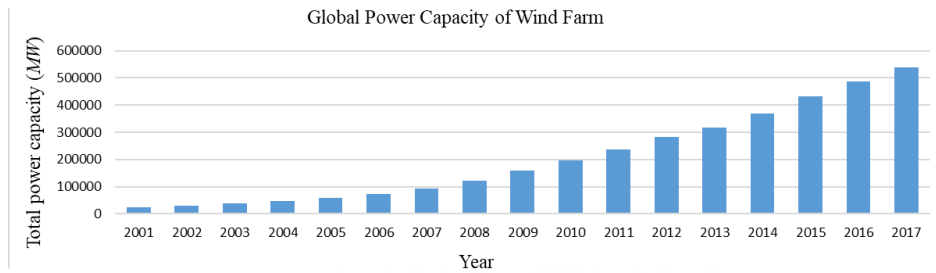


Figure 1.2 Annual global total capacity of installed wind farm from year 2001 to year 2017

Source: GWEC (2017)

One of the most significant problems that needs to be addressed is wake interaction. Wake interaction between wind turbines is currently viewed as the most challenging problem in the optimization of wind farms. Figure 1.3 shows the occurrence of wake interaction between wind turbines, whereby the blue arrow represents the incoming wind and wake is generated by each wind turbine as the wind blows. As a result, the wake of the upstream turbines will directly affect the performance of its corresponding downstream turbines, chaining the effect towards the turbines in the final row. This would eventually create a hierarchy of complex interaction among all the wind turbines throughout the wind farm. In order to further understand the effect of the wake, an analysis of wake interaction is shown in Figure 1.4. As noted, the highest, moderate and lowest wind speeds are indicated with red, green and blue colors, respectively. Initially, the wind has the highest speed before passing through any wind turbine. Yet, it is degraded to a moderate speed when passing through wind turbines in the first row, causing the wind experienced by the downstream wind turbines to be at the lowest speed. This effect would continue to affect the other wind turbines downstream, causing an inconsistent wind pattern throughout the wind farm. With this, this figure has illustrated the difficulties in understanding the wake dynamic due to the complex interaction between wind turbines.

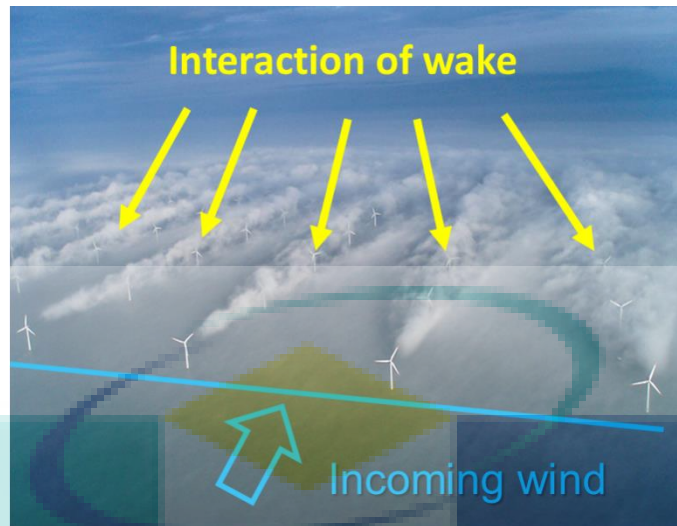


Figure 1.3 Wake interaction among wind turbines in wind farm  
 Source: Joshua S Hill (2017)

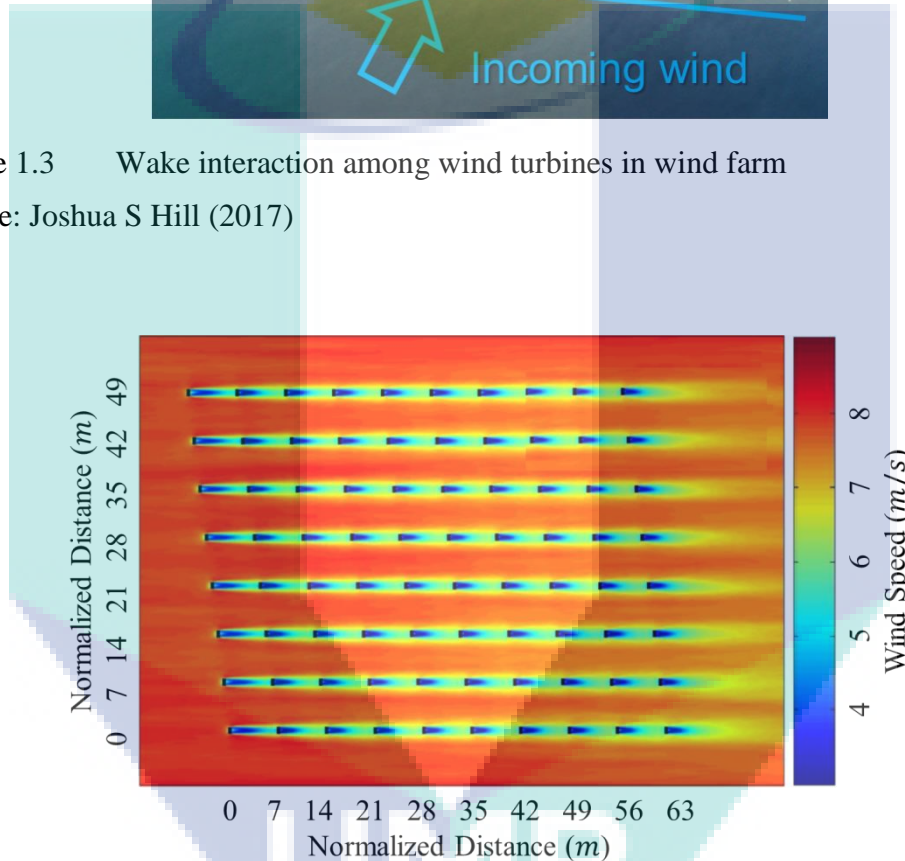


Figure 1.4 Analysis of wake effect between wind turbines in wind farm  
 Source: Porté-Agel *et al.* (2013)

Within the effort to improve the total power production of wind farms, two prevalent research problems are highlighted, which are the problems in micro-siting and the axial induction factor (controller) optimization.

### 1.1.1 Micro-siting Optimization of Wind Farm

Micro-siting optimization is a method used to evaluate the optimum number of wind turbines and the positioning of each wind turbine in the wind farm towards reducing the

cost of power production, while increasing the total power produced (Yin *et al.*, 2017). This problem usually emerges when wind farms are to be newly installed in specific locations. Herewith, micro-siting would need to overcome the problems presented by wind dynamics since it is based on static wind models such as the wind rose model, which demonstrates no information on dynamic wind (Mosetti *et al.*, 1994). As illustrated in the example of a wind rose model in Figure 1.5, micro-siting optimization is developed to resolve the problems affected by wind dynamics, in order to increase the performance of a wind farm.

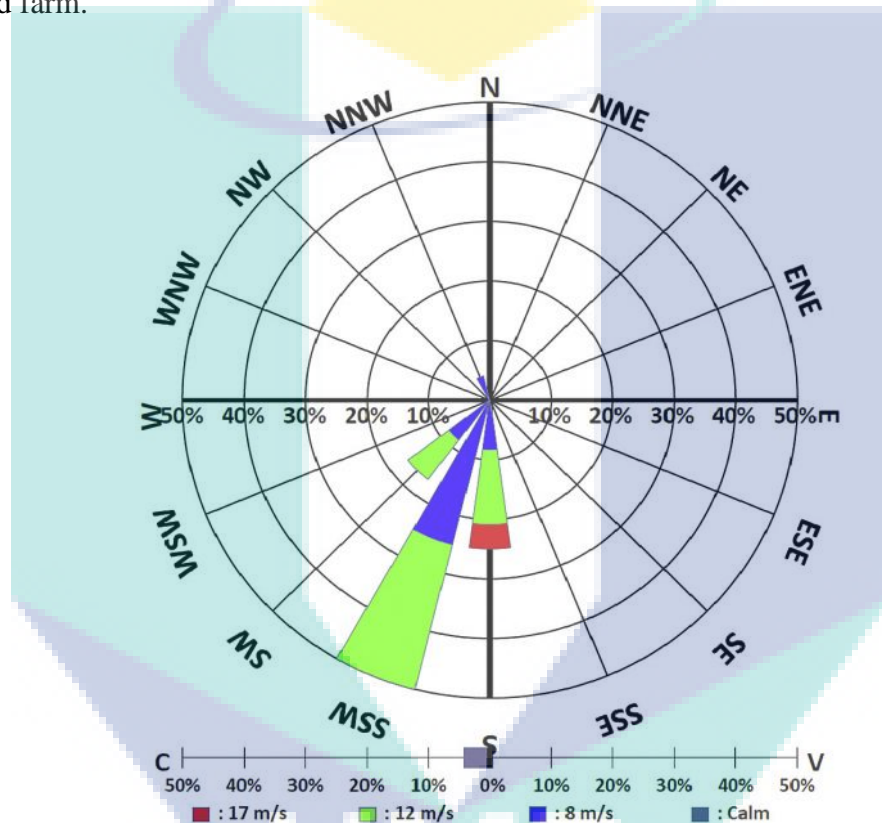


Figure 1.5 The indication of wind speed and direction occurrence frequency known as a wind rose

Source: Yin, Wu and Hsu (2017)

### 1.1.2 Axial Induction Factor (Controller) Optimization of Wind Farm

A controller or axial induction factor optimization is a method used to tune the control parameters of each wind turbine in a wind farm, to maximize the total power production based on the wind dynamics. Normally, controller optimization is carried out for an existing wind farm, rather than to be newly installed. This occurs when the optimum controller of a standalone wind turbine is no longer working among an array of

turbines due to the wake interactions between turbines. Therefore, re-tuning will need to be done towards the existing optimum controller of that standalone turbine, so as improving the total power produced by the wind farm.

However, the model-based approach is difficult to establish due to the complexity and uncertainties of the wake effect (Marden *et al.*, 2012). Not to mention, the establishment of a model-based approach is time-consuming due to the lengthy time the wind requires to travel throughout the wind farm (Gebraad *et al.*, 2013; Ahmad *et al.*, 2014). On the other hand, the model-free approach would be more practical as it does not require any explicit form of wind farm model. For example, Figure 1.6 shows the generic optimization block diagram of a model-free approach. In the figure, the specific model of system remains unknown and optimization is carried out only based on the information of input and output, further avoiding the difficulties and uncertainties of wind farm modelling.

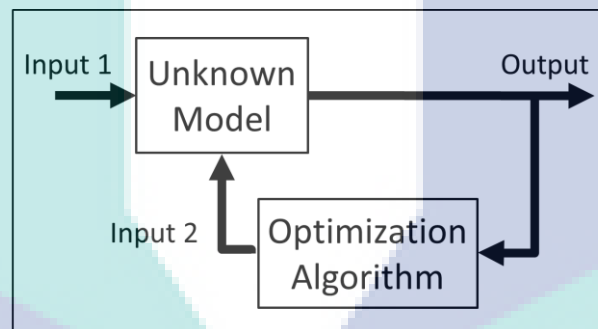


Figure 1.6 Generic optimization block diagram of model-free approach.

## 1.2 Motivation and Problem Statement

On one hand, Multi-agent optimization methods (MAOM) such as Particle Swarm Optimization (PSO) (Chowdhury *et al.*, 2012) and Spiral Dynamic Algorithm (SDA) are more preferable for offline optimization due to their ability in providing highly accurate output. However, due to vast amount of computation effort required, MAOM have a slow convergence rate, making them unsuitable for real-time applications. On the other hand, single-agent optimization methods (SAOM) such as Random Search (RS) only require one evaluation process in the searching of optimum objective function, which can provide reasonably accurate outputs in a short period of time. Yet, based on our preliminary study, the conventional RS remains incapable of improving total production with reasonable

convergence rate. For instant, in the case of the Horns Rev wind farm with 80 turbines (Kristoffersen *et al.*, 2003), the conventional RS requires more than 100 hours to maximize its total power production. Having the possibility of wind condition to change within an hour, this convergence rate would be impractical to apply for the total power optimization of real-time wind farms. The detail is shown in Mohd (2015), whereby the convergence speed is degraded when a higher dimensional design parameter is adopted.

In Ahmad *et al.* (2014), a Multi-resolution Simultaneous Perturbation Stochastic Approximation (MR-SPSA) was introduced to solve the convergence rate issue while maximizing total power production. However, this approach still presents less accuracy towards maximizing total power produced due to its memory-less structure. Moreover, the MR-SPSA is also unable to save the best optimum values during the tuning process. With such limitations, this makes memorisable algorithms such as the RS a better option to be explored. Provided that the output fitness is improved, RS would be able to update the objective function in the next iteration. In the context of exploiting wind energy, multiple variations of RS based algorithms can be an interesting field of study, further exploring their potential in optimizing large scale wind farms for power production.

Previous studies based on a various type of RS-based methods such as Fixed Step Size Random Search (FSSRS), Adaptive Step Size Random Search (ASSRS), Sequential Random Search (SRS) and Optimized Relative Step Size Random Search (ORSSRS) had shown that ORSSRS has the most promising performance to optimize large scale wind farm, due to its ability to produce the highest and most stable total power production among all the RS-based methods. While ORSSRS evaluates all possible steps around the current solution to perform optimization, this approach does not fulfil the requirement of real-time optimization as the simulated optimization has required more than 100 hours to be completed. Therefore, the dimension number of problems is significantly affecting the overall convergence time of ORSSRS. Consequently, it is necessary to improve the convergence time of ORSSRS for real-time optimization of wind farm, while maintaining the ability to produce maximum total power production.

### **1.3 Objectives**

The main objectives of this research study are:

- I. To develop a Multi-resolution Optimized Relative Step Size Random Search (MR-ORSSRS) for real-time wind farm power production optimization.
- II. To evaluate the robustness of MR-ORSSRS in term of different wind directions, wind speed, and wind turbine failure.
- III. To compare the performance of MR-ORSSRS with other existing methods in term of its convergence rate, and the maximum total power production.

#### **1.4 Scope and Limitations**

This research is mainly focused on the optimization of power production in a model-free wind farm. The result validation is based on the real-time wind farm dynamic model employed by Horns Rev wind farm in Denmark, as proposed by Gebraad *et al.* (2013). The wind farm system, including the wake expansion and decay of wind speed due to the wake effect, is referred to as the Park Model (Porté-Agel *et al.*, 2013). It also includes the addition of a delay structure to illustrate the real situation of wind transition. Meanwhile, the term ‘model-free’ means that optimization is carried out based only on the input and output data of the wind farm model. Herewith, several variants of the Random Search methods are tested to optimize the power production of the wind farm. The best Random Search method would then be selected to hybrid alongside the multi-resolution functions. Following this, as demonstrated by Ahmad *et al.* (2014), the results will be compared to the existing MR-SPSA for the wind direction variation at the angle of 170°, 200°, 220°, 240°, 250° and 270°, since the wake effect is utmost significant at these angles. Time-varying (wind direction and speeds) and wind turbine failures are further compared in the results.

#### **1.5 Overview of the Thesis**

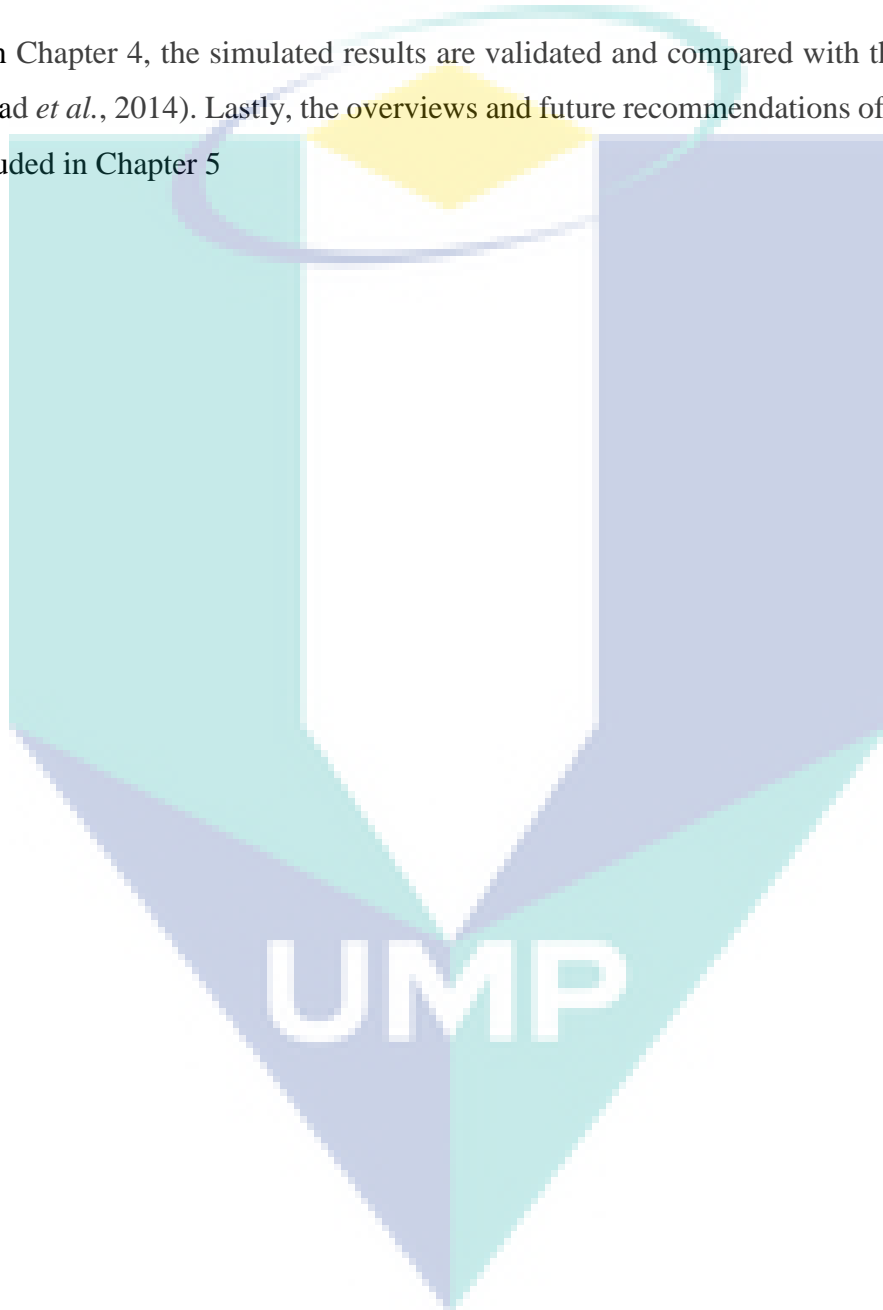
The brief introduction of wind farm optimization was presented in Chapter 1, where the problems and objectives have been clearly stated.

Chapter 2 presents a comprehensive overview of the literature related to this study. The literature includes wind farm optimization techniques, design approaches and optimization methods which are variables that will be investigated in the current study.



The methodology is presented in Chapter 3 where the algorithmic steps and problem formulation are discussed in detail. An in-depth explanation on the operations of the ORSSRS is presented, and the function of Multi-resolution is well illustrated. Subsequently, a dynamic wind farm model will be formulated based on the Horns Rev wind farm model as proposed by Gebraad *et al.* (2013).

In Chapter 4, the simulated results are validated and compared with the MR-SPSA (Ahmad *et al.*, 2014). Lastly, the overviews and future recommendations of the study are concluded in Chapter 5



## CHAPTER 2

### LITERATURE REVIEW

#### 2.1 Introduction

Existing wind farm optimization techniques and methods are reviewed, and being discussed in this chapter. First and foremost, the optimization of micro-siting planning is discussed in Section 2.2. Due to some existing limitations, controller optimization is introduced in two approaches, which are the model-based and the model-free approaches. Both approaches are studied and summarized in Section 2.3 and Section 2.4, respectively. Lastly, Section 2.5 summarizes the reviewed approaches and methods. Figure 2.1 presents the overview of the literature reviewed for this study.

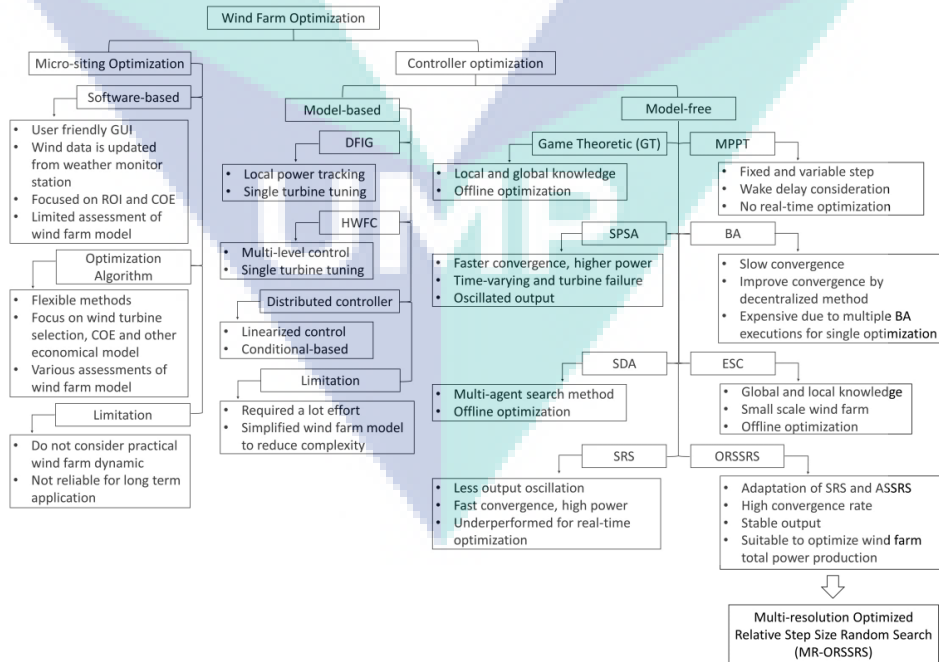


Figure 2.1 Summarized reviews of related literature of this study.

## 2.2 Micro-siting Optimization

Micro-siting planning is crucial towards the development of new wind farms. It is used to forecast the potential wind power extraction on the landscape, in minimizing the wind farm installation costs, while maximizing the total energy produced annually. The literature regarding micro-siting planning of wind farms is briefly reviewed in this section.

### 2.2.1 Software-based Optimization

There are several software packages developed to assess micro-siting performance of wind farms. WAsP (Sveinbjornsson, 2013) is the most popular among the micro-siting performance assessment software. This software mainly focuses on wind resource assessment, basing its assessment on the wind data obtained from nearby meteorological stations. With this, it is able to predict the amount of wind resource within a landscape; yet, unable to provide an accurate measurement due to complexity of the terrain. In resolution, a later version of the software, WAsP 11 has included a new feature that allows micro-siting performance of wind farm on complex terrain to be assessed, through using the Computational Fluid Dynamics (CFD). This software is also implemented with measurement of extractable wind power due to the placement of wind turbines, as according to the Katic model (Katic *et al.*, 1986). Another similar software is Wind Sim (Serrano Gonzalez *et al.*, 2014). This software focuses on determining the best placement of wind turbines in order to get the best wind condition on complex terrain. Herewith, A 3D Reynolds-averaged Navier–Stokes solver based CFD model is included in the assessment of wind resource. These two software packages mainly focus on the evaluation of wind resource on a landscape, which prove important for developers to forecast and utilize the available wind power through confirming the wind frequency of the landscape. However, noted that these software do not provide information regarding optimum wind turbines placement towards optimizing the total power production of wind farms.

Nevertheless, there are other software packages that provide assistance towards the optimization of wind farms such as Wind Farmer (Vincent, 2009), Wind Pro (Nielsen, 2013) and Open Wind (Truepower, 2010). The optimization via these software are based on different objectives. As such, Wind Farmer optimizes wind turbines placement to

obtain maximum return on investment (ROI). It also includes the wake effect based on the Reynolds-averaged Navier–Stokes solver CFD model. However, the detail of optimization method implemented in this software remains unknown. On the other hand, Wind Pro evaluates the optimization quality based on the total annual power production, whereby the wake effect is based on the Katic model (Katic *et al.*, 1986). Meanwhile, the wind turbines placement optimization policy can be both random and symmetrical. Alternatively, the micro-siting optimization is carried out in Open Wind by referring to the cost of energy (COE), with the wake effect also based on the Katic model (Katic *et al.*, 1986). The software-based wind farm micro-siting optimization is user-friendly with the Graphical User Interfaces (GUI) as shown in Figure 2.2 and Figure 2.3. For example, the GUI in Figure 2.2 has a good presentation of wind turbines arrangement with different viewing perspectives, which allows user to visualize the arrangement results of wind farm. Whereas, the GUI in Figure 2.3 has a good illustration of landscape terrains and wind rose, which allows users to identify the power production efficiency and effective wind directions on the landscape. Consequently, GUIs are useful to investigate the fitness of a landscape for the purpose of wind farm development.

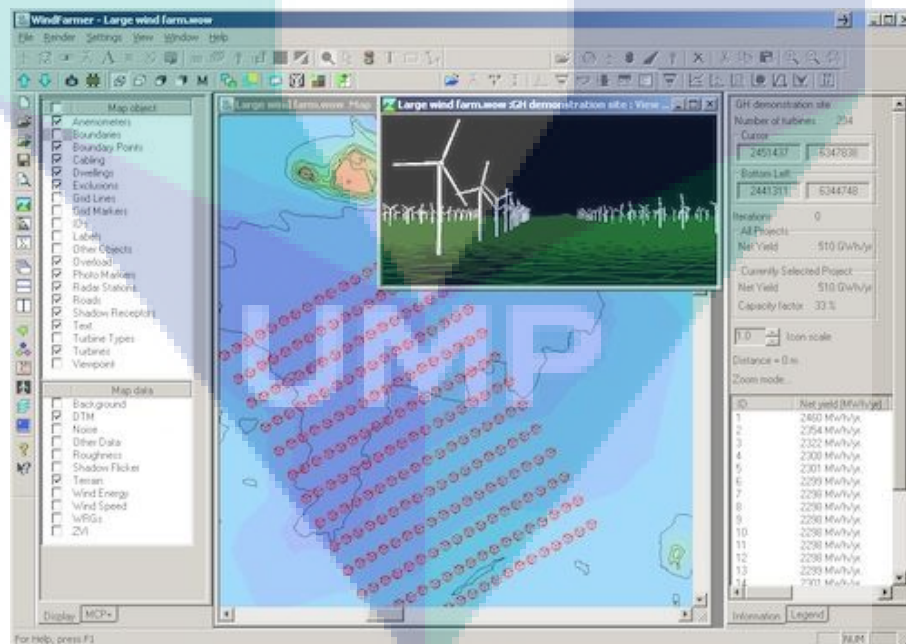


Figure 2.2 GUI of Wind Farmer 4.2 wind from micro-siting optimization software with the illustration of wind farm layout and the appearance of with turbines arrangement.  
Source: Herman (2011)

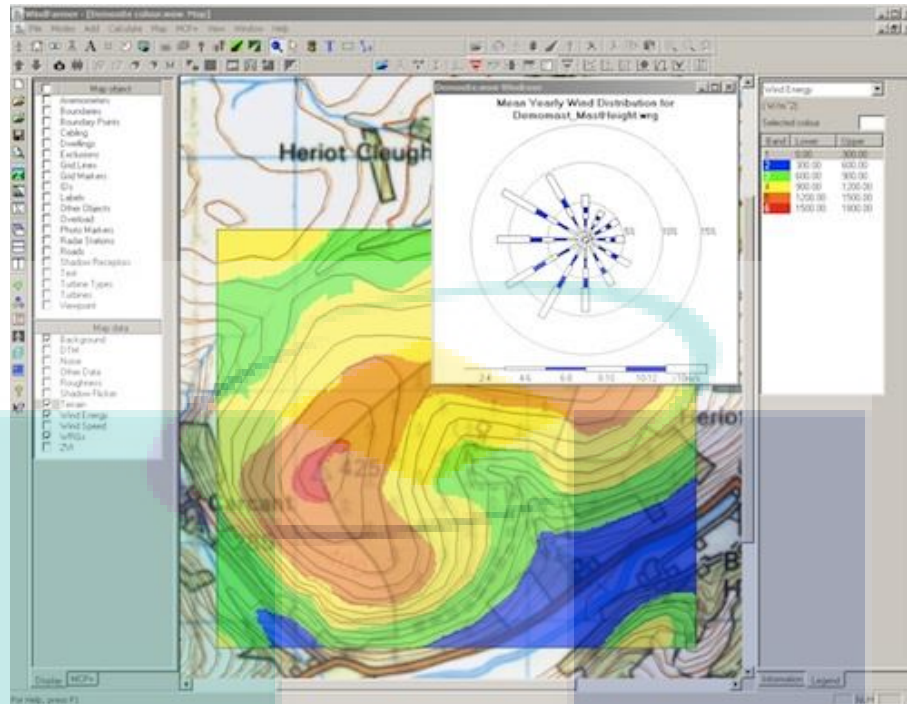


Figure 2.3 GUI of Wind Farmer 4.2 with the illustration of wind speed and direction according to the wind data acquired from wind rose model

Source: Herman (2011)

However, the software packages mentioned above are not available for advance investigation. As previously noted, each of these software packages focuses solely on one optimization objective and most of them use the Katic model as the basis for their wake effect. Therefore, users are unable to explore extensive details including dynamic and static wake effect comparisons, multi-objective optimization and the effectiveness of optimization algorithms, towards evaluating the fitness of landscape for wind farm development. This has entailed more investigations and reporting conducted on micro-siting optimization of wind farms by other scientific journals.

## 2.2.2 Optimization Algorithms

Genetic Algorithm (GA) is the most studied algorithm in the optimization of wind farm micro-siting. The investigation on economical improvement of wind farms through micro-siting optimization was initially proposed by Grady *et al.* (2005). Later, the study was extended by implementing a considerably complex economic model, as proposed by Mora *et al.* (2007). A model-free approach of the similar study was then proposed in Marmidis *et al.* (2008). An investigation on the levelized cost of energy (LCOE) in the

case of offshore wind farms was also suggested in Elkinton *et al.* (2008). Furthermore, Şişbot *et al.* (2010) has recommended a multi-objective wind farm micro-siting optimization, where the objectives aim to maximize the annual power production and minimize the cost of energy. Besides GA, the performance of wind farm micro-siting optimization was also investigated by using other optimization algorithms. Among others, Particle Swarm Optimization (PSO) algorithm was proposed to optimize wind farm micro-siting in a continuous way (Mora *et al.*, 2007). This method was used to choose the best combination of wind turbine model and diameter on a given landscape in order to maximize power production (Mustakerov *et al.*, 2010). Besides, Wan *et al.* (2012) further introduced the innovative Gaussian Particle Swarm Algorithm (GPSO) to optimize the problem highlighted by Mora *et al.* (2007). In view of a multi-objective approach, Strong Pareto Evolution Algorithm (SPEA) had also been implemented in the micro-siting optimization of wind farms; yet, with the argument presented by Bazacliu *et al.* (2015), stating that continuous computation domain should be used in the process of optimization shall SPEA is implemented.

### **2.2.3 Limitation of Wind Farm Micro-Siting Optimization**

Micro-siting optimization of wind farms is useful for new wind farm development as it can assist in forecasting the wind power availability of the landscape, providing the best wind farm layout solution within complex terrains and evaluating minimum installation cost towards obtaining the highest power production profit (Serrano Gonzalez *et al.*, 2014). However, it is not adaptive to chaotic weather changes and wind disturbance such as wind gust and hurricane, as well as the occurrence of turbine failure, which would reduce the optimization efficiency (Spudic, 2010). The potential of improving the performance in term of real-time tuning has led to new research efforts in controller optimization. Many approaches to optimize the controller of wind turbines have been established. The model-based approach is carried out according to actual conditions of existing wind farms, while the model-free approach is established based on the input and output information of wind farms.

## **2.3 Model-based Controller Optimization**

The controllers reviewed in this section are model-based optimization. Researchers often try to design the optimization controller according to a real wind farm. Normally,

these controllers are designed for wind farm development projects such as the Horns Rev wind farm in Denmark (Kristoffersen *et al.*, 2003), the Yerga wind farm in Spain (Dash, 2002) and the Aeolus wind farm in Canada (Spudic, 2010). As such, These controllers can work towards optimizing power production of the dedicated wind farm.

### **2.3.1 Doubly Fed Induction Generation (DFIG)**

DFIG is a model-based controller which can optimize power production of each turbine in a wind farm. As mentioned earlier, it is applied on the Horns Rev wind farm in Denmark (Kristoffersen *et al.*, 2003) and the Yerga wind farm in Spain (Dash, 2002). The controller is mainly used to detect turbine's fault which would cause the lost of power production due to wound rotor induction generator. In accordance to the current wind condition, this controller enable adjustments to the control parameter such as the faulty turbine's yaw angle and rotor blade's pitch angle to obtain the desired power production. However, with DFIG being a single turbine controller, it is unable to maintain the total power production of a wind farm if the faulty turbine is heavily wounded or damaged, thereby resulted total power production lost. On the other hand, centralized power control of DFIG as proposed by Hansen *et al.* (2006), harnesses the ability of DFIG to maintain total power production of a wind farm with a centralized power controller. Following this, the DFIG monitors then change in active power and reactive power produced by the wind turbine generator, further obtain the available power of each turbine. Subsequently, the available power production is fed back to the central controller, where it will decide whether to adjust the control parameter of wind turbines in compensating for the power lost. The proposed method has shown promising results in controlling the power production of the wind farm. However, the results in a study conducted by Hansen *et al.* (2006) have only based on a simplified wind farm with three wind turbines. Therefore, the ability to tune high-dimensional parameter is yet to be defined.

### **2.3.2 Hierarchical wind farm control (HWFC)**

HWFC was first introduced by Spudic (2010) and was designed for the Aeolus wind farm development in Canada. The hierarchical controller is a multi-level controller, consisting of a decentralized low-level controller and a centralized high-level controller. The low-level controller has a higher adjustment rate used to readjust each wind turbine quickly upon unpredictable disturbances such as sudden wind gust and turbine failure, in

order to maintain power production of the corresponding wind turbine. Yet, the control of this level solely provides nominal adjustment, since it is a single turbine controller. Hence, in the effort to ensure accurate adjustments applied in accordance to the power reference of the wind farm, a high-level controller is further used to tune the turbines within the wind farm thoroughly. High-level controller has a comparatively lower adjustment rate, as it takes into account varying of the wind propagation due to wakes along the period of time.

Meanwhile, a similar method by Spudic *et al.* (2011) was proposed with wind turbine structural stress consideration. In this case, a turbine rotor rotational speed and a turbine shaft moment stress are used as the power feedback. The low-level controller is used to monitor the wind speed and turbine shaft moment in deciding the desired rotor rotational speed, which then manipulates the blade pitch angle of the corresponding wind turbine. Meanwhile, the high-level controller monitors the overall power production of the wind farm and controlled each wind turbine to extract the available power according to its power reference. This way, both the structural stress of each wind turbine and the power production of the entire wind farm can be maintained. Thus, the method proposed in Spudic *et al.* (2011) can simultaneously reduce wind turbine maintenance cost, while sustaining power productivity. However, the multi-level controller method requires increased computation effort to carry out the optimization, making it inefficient for large-dimensional parameter tuning.

### **2.3.3 Distributed Controller**

The distributed controller is designed to reduce the load of wind turbines in wind farm, by evenly distributing the load throughout all the wind turbines within a wind farm. With all the turbines equally sharing the total load, turbine stress is reduced while power production is maintained. The distributed control was introduced by Soleimanzadeh *et al.* (2011), who have proposed two control strategies, namely low-wind speed and high-wind speed. On this note, high-wind speed has applied the linearized wind propagated wake model for the purpose of power and stress prediction. Whereas, wind turbines can extract maximum available power at low-wind speed, with the turbine structural stress being minimized in this state. Herewith, it is mentioned the wake interactions among the wind turbines, where the power generated by a turbine is not only affected by the control parameter of itself, but also the control parameter of both the upstream and downstream



turbines. Another similar research has applied linear-quadratic regulator (LQR) controller (Soleimanzadeh *et al.*, 2012) based on NREL 5MW wind turbine (Jonkman *et al.*, 2009). The LQR obtains wind prediction from the linearized wind propagated wake model and wind farm power reference, towards deciding the power distribution for each turbine in the wind farm. The results have been presented based on a wind farm with an array of five wind turbines, which shows that LQR is the best method to distribute the load of a wind farm to all the turbines evenly, as compared to the numerical method and the controller-less wind farm model.

#### **2.3.4 Limitation of Model-based Approaches**

Model-based approaches can provide the exact solution for wind farm optimization. However, it is only limited to the dedicated wind farm and wind turbine. This suggests that their optimization are targeted to single-turbine tuning, as proposed by Hansen *et al.* (2006) and Spudic (2010) who have presented a lack of effective communication between wind turbines due to the wake effect. Moreover, the development of model-based approaches require considerable time and efforts, as it accounts for the analysis of wind farm behaviour such as the wake interaction between wind turbines. Therefore, small-scale wind farm is always preferred in the application to minimize the complexity for optimization. For these approaches, Hansen *et al.* (2006) has presented optimization based on a simplified wind farm consisting of an array of three wind turbines; while Soleimanzadeh *et al.* (2012) has proposed optimization based on a single-array wind farm of five wind turbines. Noted that existing wind farms are built on a large-scale consisting of multi-array of multiple wind turbines, model-based approaches would not be suitable within this context.

#### **2.4 Model-free Controller Optimization**

The uniqueness of a model-free based optimization is its data-driven characteristic. This optimization can be carried out without the need of modelling the system, as it based its algorithm on the input and output data of the system, as illustrated in Figure 2.4. Noted that the effort for system analysis and modelling is not required in this approach, further simplifies the optimization development. However, the significance of the optimization efficiency relies on the convergent rate of the optimization methods. Following are the

reviews of existing model-free approaches that optimize the total power production of wind farms.

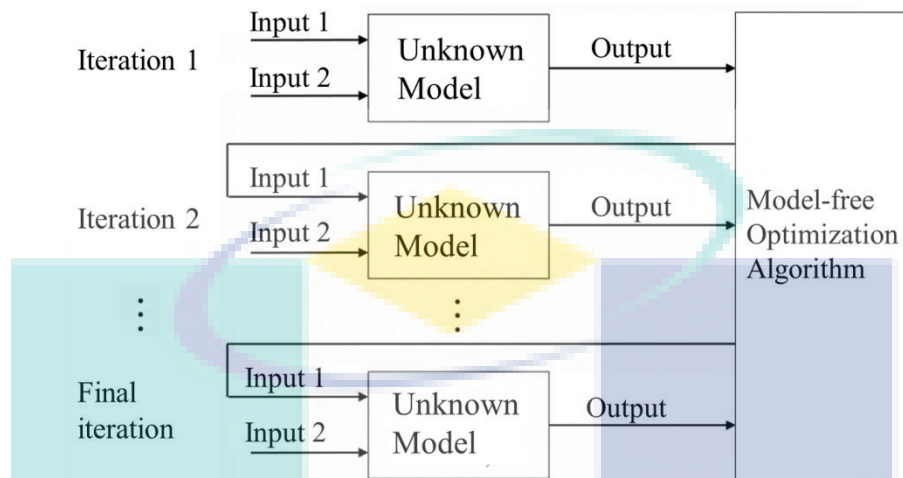


Figure 2.4 An example of model-free optimization approach based on the information of input and output.

#### 2.4.1 Game Theoretic (GT)

The first model-free approach wind farm optimization using GT has been proposed by Marden *et al.* (2012), and an extended study is further conducted by Marden *et al.* (2013). The performance between the two GT-based distributed learning algorithms, known as safe experimental dynamics (SED) and payoff-based distributed learning for Pareto optimality (PDLPO) was also compared by Marden *et al.* (2013). The differences between the learning algorithms are global and local knowledge-based optimization. In SED, knowledge on the total power production of wind farms is shared among each of the wind turbines. On the other hand, PDLPO solely demonstrates that each individual wind turbine only assess its own power production, with limited knowledge on the power production of neighbouring wind turbines. Comparatively, the results has shown that SED can entail the optimization towards a higher total power production of a wind farm, as compared to PDLPO. Furthermore, a different type of GT was proposed by Park *et al.* (2013), where the control relations between the wind turbine yaw-angle offset and axial induction factor to maximize total power production of the wind farm has been utilized. The results were compared with the Non-cooperative Game and Cooperative Game control methods. In the Non-cooperative Game control method, the objective is distributed to each of the wind turbines individually; whereas, all the wind turbines in Cooperative Game control method share the same objective as a whole. Eventually, the

Cooperative Game control will have a better performance than the Non-cooperative control, in term of maximizing the total power production of the wind farm.

The proposed studies mentioned above have presented the comparison between the local and global maximization of wind farms' total power production. However, the optimization are validated based on the static wind model. Being an offline optimization method, its reliability for real-time optimization remains unknown.

#### **2.4.2 Maximum Power Point Tracking (MPPT)**

The performance of MPPT optimization methods is investigated, in order to be applied in the real-time optimization of wind farms. The MPPT method was proposed by Gebraad *et al.* (2013) using a dynamic wind farm model, where the wake delay generated by the wind turbines was approximated in the optimization process. In this context, the authors compared performance of Fixed Step Maximum Power Point Tracking (FS-MPPT) with the Gradient-Descent Maximum Power Point Tracking (GD-MPPT) on maximizing the total power production of wind farms. Results show both MPPT-based variations can produce a higher power with faster convergence rate, as compared to GT. However, the power production optimized by FS-MPPT fluctuates around the optimal power production, due to its fixed-step characteristic. GD-MPPT, on the other hand, can perform better in reducing the power oscillation as compared to the FS-MPPT. Nevertheless, this study only covers the varying time effects of the wake; while the ability to recover from an unlikely event such as wind turbine failure is more crucial to be evaluated than the performance of real-time optimization.

#### **2.4.3 Simultaneous Perturbation Stochastic Approximation (SPSA)**

The preliminary investigation on real-time optimization of the wind farm's total power production was reported by Ahmad *et al.* (2014) based on the dynamic wind farm model proposed in Gebraad *et al.* (2013); whereby the wake delay generated from a wind farm to another was approximated. In this study, optimization was carried in a distributed manner to achieve global maxima. However, the wind farm validated in this study was a simplified, single array wind farm consisting of four wind turbines, so as to reduce the complexity of the investigation. Comparing its performance to GT (Marden, Ruben and Pao, 2013) and FS-MTTP (Gebraad *et al.*, 2013), results show that SPSA enables

maximum total power production of the wind farm, topping those of the fore-mentioned methods, as it can provide a faster convergence speed.

However, the capability of SPSA to optimize a large-scale wind farm was undefined as the validation was conducted only upon a simplified single array wind farm. This called for a more extended study of this application (Ahmad *et al.*, 2014). In this case, the SPSA optimization method was modified into Multi-Resolution Simultaneous Perturbation Stochastic Approximation (MR-SPSA) in order to further improve the convergence rate. A dynamic wind farm model consisting of 80 wind turbines based on the Horns Rev wind farm in Denmark has been used to validate its performance, in term of wind speed and direction variations. To consider the real-time optimization constraints, the validation of time varying and turbine failure were further included. In comparing its performance with GT (Marden *et al.*, 2013), FS-MTTP (P. M. O. Gebraad *et al.*, 2013) and SPSA (Ahmad *et al.*, July 2014), MR-SPSA had successfully optimized the wind farm's total power production with a higher convergence rate and capability for real-time optimization. Yet, it was unable to provide a stable optimal results due to the memory-less characteristic of MR-SPSA. Thus, this makes the use of memorisable optimization methods such as Bayesian Ascent (BA) and Random Search (RS) more preferable.

#### **2.4.4 Bayesian Ascent (BA)**

A concept investigation of the wind farm's total power production optimization using BA was proposed by J Park *et al.* (2016). The BA was developed based on the Bayesian Optimization (BO) method, with the implementation of a trust region method to increase the search-ability of the BO-based algorithm. This is because BO tends to search for the optimum input in large input space, which may cause ineffective convergence. In this study, the concept was tested to optimize a single array wind farm with three wind turbines in both the cooperative and greedy modes.

Cooperative mode is the global optimization where the wind turbines are cooperatively controlled to maximize the overall power production of the wind farm; whereas, greedy mode is the local optimization where the wind turbines are set to extract wind power at a maximum capacity. Eventually, BA can increase the total power production of the wind farm by 27% as compared to the greedy mode. Jinkyoo Park *et al.* (2016) further extended the investigation of BA to optimize a large-scale wind farm

under dynamic wind conditions such as the variations in wind speed and direction. Yet, with BA unable to optimize large dimensional problem, the authors subsequently proposed the use of a decentralized method to increase the rate of convergence, through defining the wind farm into clusters of wind turbines. BA algorithm was then applied to each cluster to maximize the power production of the wind turbines in that cluster, equivalent to a single array wind farm optimization. Nevertheless, with multiple BA algorithms required for each optimization, this method has been found to be expensive in execution. Hence, optimization methods with high convergence rate such as Random Search (RS), would be a comparatively better application option within this context.

#### **2.4.5 Spiral Dynamic Algorithm (SDA)**

A preliminary investigation of the wind farm's total power production optimization using SDA has been proposed and conducted in a previous study, based upon a single-array wind farm consisting of ten wind turbines. In this field of study, the performance was compared in term of total power maximization with other multi-agent based optimization methods, namely PSO and GT. Through the study that focused on offline optimization, SDA was shown to produce a higher total power production, as compared to PSO and GT. Yet, noted that offline optimization does not account for the convergence rate, which presents vague guarantee on the validity of the SDA application in real-time wind farm optimization.

#### **2.4.6 Extremum-Seeking Control (ESC)**

The investigation towards the optimization of total power production using ESC via a model-free wind farm model was initially reported in a study by Ciri *et al.* (2017). This study accounted for the comparison between performances of both Individual ESC (IESC) and Nested EST (NEST). IESC has been known to operate based on greedy optimization, with the power production of each turbine in the wind farm individually tuned to extract the maximum available wind power. Meanwhile, NEST operates using global optimization, where every wind turbine in the wind farm is cooperatively optimized with careful consideration of the wake effect to maximize the total power production throughout the wind farm. Based on the findings, it is deduced that the wake delay due to wind transitions from the upstream to the downstream wind turbines had been extensively studied in Ciri *et al.* (2017). However, take note that the results were

obtained based on a single array wind farm with three turbines. Indirectly, the study might have overlooked the ability of ESC in optimizing a large-scale wind farm.

#### **2.4.7 Random Search (RS)**

The preliminary investigation of the RS-based method to optimize the wind farm power was reported in a previous study by Marden *et al.* (2013). Here, the standard Sequential Random Search (SRS) was applied, and its performance was then compared with GT (Marden *et al.*, 2013). The validation was carried out based on the Horns Rev wind farm in Denmark, consisting of 80 wind turbines, while taking into considerations wake interactions among the wind turbines. With this, SRS was shown to provide a higher power production with a faster convergence rate. The output was also found to be highly stable where the standard deviation of power production was recorded at only  $0.627 \times 10^{-3} MW$ , compared to 2.172 MW in GT. With regards to such findings, the RS-based optimization method presents promising prospect to optimize a wind farm's total power production in a model-free approach. This entails the potential for further investigation on the capability of RS-based methods for real-time optimization.

#### **2.4.8 Optimize Relative Step Size Random Search (ORSSRS)**

The performance of Random Search-based algorithm on the optimization of a wind farm's total power production has been investigated in a previous study. In particular, the study based its evaluations on a static wind farm model, where the dynamic wake interaction between the wind farms was not included. Meanwhile, the investigated algorithms used were the Fixed Step Size Random Search (FSSRS), Adaptive Step Size Random Search (ASSRS), Sequential Random Search (SRS) and Optimize Relative Step Size Random Search (ORSSRS) based on the Horns Rev wind farm in Denmark. FSSRS is the fundamental RS-based algorithm; yet, extensive care required to define the step size has presented difficulties for its implementation. Step size is proven to be important, as it can affect both the convergence time and the stability of total power production. For example, a big step size can result in faster convergence time with higher fluctuations in total power production; conversely, small step size entails more stable power production with the requirement of a longer convergence time. Therefore, ASSRS was introduced to resolve the problem of FSSRS, by comparing the fitness of the total power productions acquired in two steps with different sizes (Schumer *et al.*, 1968). Emphasis on the big

step size can improve the convergence time, while focus on the small step size can improve stability in total power production. However, ASSRS requires more monetary spending in evaluating multiple total power production within each iteration, making this approach less cost effective.

On the other hand, the step size of SRS is iteratively reduced in every iteration to minimize the overall power production fluctuation at the end of the optimization. Having said that, the step size reduction policy is sensitive to the overall performance of the SRS. Overly rapid reduction of step size would cause difficulties towards achieving the optimum level in total power production; whereas, overly slow reduction in step size would require a longer time to achieve a steady total power production. Alternatively, the ORSSRS would optimize the step size reduction policy of SRS by adapting the fitness evaluation of total power production from ASSRS, whereby the step size is reduced according to the fitness of the total power production in every iteration, such that the step size is only reduced if the total power production is higher than the ones in the previous iteration. Therefore, ORSSRS can produce the highest and the most stable total power production, with the fastest convergence speed among tested RS-based algorithms. Based on the findings, it is deduced that ORSSRS would be the most suitable optimization algorithm to optimize the total power production of a wind farm based on the static wake model.

## **2.5 Summary**

Many efforts have been carried out to improve a wind farm's performance from the beginning of construction until the end of installation. The micro-siting of a wind farm is important at the initial stage of construction as it can estimate the cost needed for power production; also known as the cost of energy (COE). Therefore, most of the micro-siting optimization for wind farms have based their objective on COE minimization. However, the optimization are based on historical static wind models which limit their reliability for long-term applications. Therefore, investigations on controller optimization have become an increasingly popular research field for the control community.

Optimization of the controller can be categorized into two different approaches which are the model-based and model-free approaches. Model-based approaches investigate the control method of a wind farm, base on existing wind farms and wind

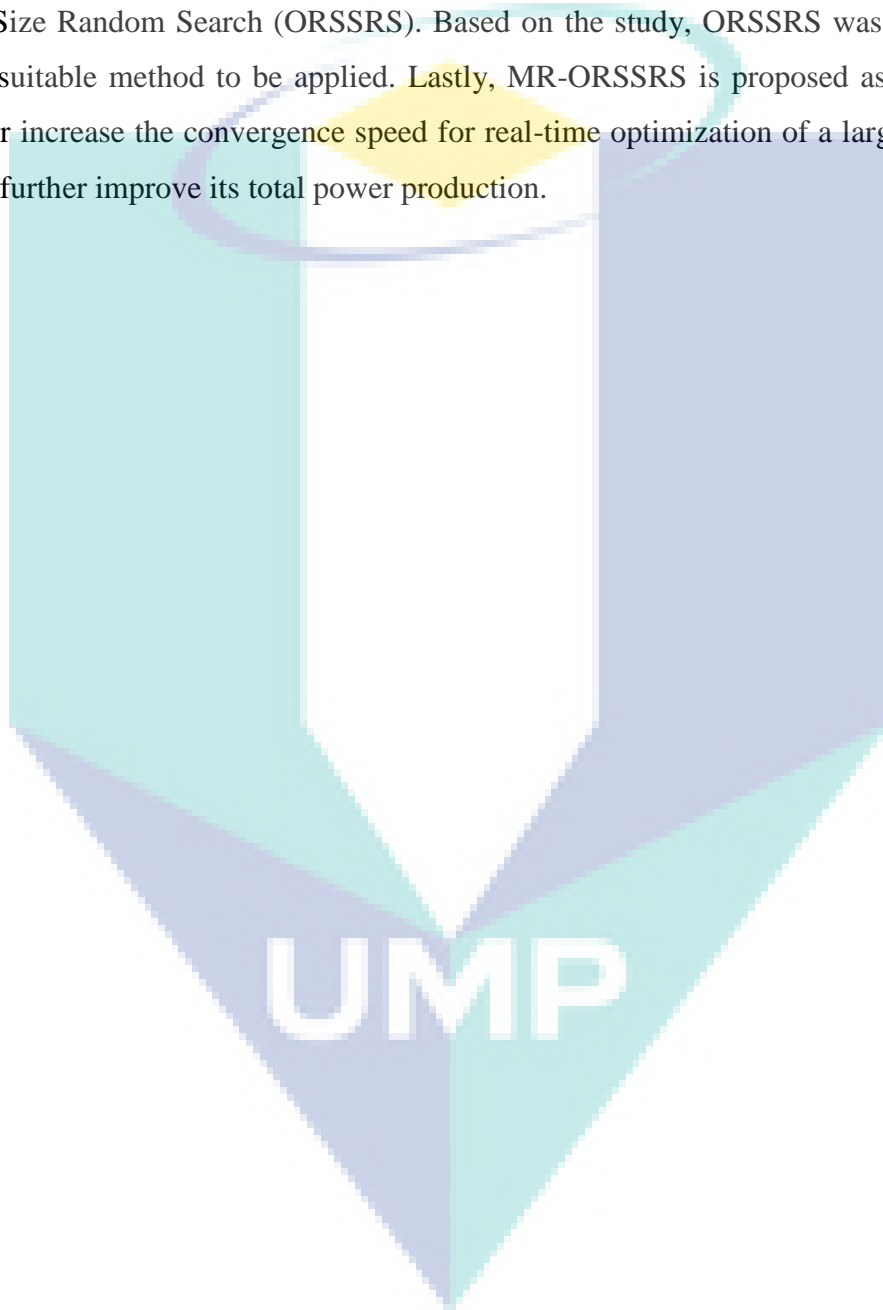
turbines. Most of the optimization focus on a single wind turbine tuning, which have resulted in an ineffective communication between wind turbines and reduced the optimization effect. Meanwhile, model-based optimization is difficult to practice as it requires considerable effort in the analysis and formulation of complex wind farm dynamics. Therefore, the proposed methods are often being validated through simplified wind farm models.

Model-free optimization, on the other hand, can be carried out without the requirements for model formulation, minimize the optimization efforts. However, the performance of optimization relies heavily on the convergence speed and output stability of the optimization methods. GT was the first method proposed to investigate the model-free approach wind farm power production. The proposed SED and PDLPO further contributed the primary ideal of local knowledge and global knowledge-based controls. Another optimization ideal was investigated by proposing two MPPT-based methods which were FS-MPPT and GD-MPPT. Here, the author compared the performance difference between fixed step and variable step algorithm in the wind farm's total power optimization. Eventually, the variable step algorithm (GD-MPPT) was found to be better than fixed step algorithm (FS-MPPT) in both higher power production and faster convergence rate. Moreover, a dynamic wind farm model with approximated wake delay to investigate the optimization performance in practical manner was established.

An advanced study to provide improvements on the convergence speed and high-dimensional parameter tuning was conducted by modifying the basic SPSA to MR-SPSA. In this study, the performance was evaluated based on an actual wind farm model. The findings further suggested that MR-SPSA was capable in producing high powered production at a faster rate. However, the output would fluctuate around the optimal, due to the memory-less characteristics of the SPSA-based methods which prefers the use of memorisable based methods. BA is one of the memorisable-based optimization methods. The authors tried to improve the convergence rate by using a decentralized method. However, it was not suitable for the optimization of actual wind farms as multiple algorithms are required to execute an optimization. Meanwhile, a preliminary investigation on SRS seems to be promising as it has the potential to produce high power production at a faster rate, as compared to GT, in the context of the Horns Rev wind farm in Denmark. However, the performance evaluation was not base on an actual wind farm



model and did not take wake dynamics into consideration. Therefore, the capability to optimize a large-scale wind farm in real-time is still far from being guaranteed. Nevertheless, further investigations on various types of RS-based optimization method continued in a later study by comparing the performance of SRS, Fixed Step Size Random Search (FSSRS), Adaptive Step Size Random Search (ASSRS) and Optimized Relative Step Size Random Search (ORSSRS). Based on the study, ORSSRS was found as the most suitable method to be applied. Lastly, MR-ORSSRS is proposed as the mean to further increase the convergence speed for real-time optimization of a large-scale wind farm, further improve its total power production.



## CHAPTER 3

### METHODOLOGY

#### 3.1 Introduction

In this chapter, a model-free optimization algorithm for maximizing the total power production of wind farm is discussed and proposed. Firstly, the wind farm system is introduced in Section 3.2, and the dynamic model of a wind farm system with wake aerodynamic interactions is presented. Section 3.3 discusses the problem formulation, which aims to find the optimal axial induction factor which ensures that the total power of wind farm is maximized.

Next, the operation of a standard Optimize Relative Step Size Random Search (ORSSRS) is reviewed in Chapter 3.4.1. In that chapter, the step-by-step operation of the algorithm is discussed. It is shown that the standard ORSSRS is capable of tuning high-dimensional parameter problem, but with an insufficient convergence speed for real-time optimization. Therefore, a Multi Resolution-Optimize Relative Step Size Random Search (MR-ORSSRS) is proposed based on a standard ORSSRS algorithm to increase the convergence speed, while maintaining the capability to solve a high-dimensional parameter problem. The operation of MR-ORSSRS is explained in Section 3.4.2. The clustering and transition of design parameters from one resolution to another and the formulation of a clustered objective function are discussed.

Section 3.5 discusses the implementation of MR-ORSSRS algorithm in maximizing the total power production of the wind farm. In particular, a step-by-step procedure of a model-free design is explained by defining the objective function as total power production and the design parameters as axial induction factors. Furthermore, the

implemented design parameters clustering technique is also explained in this section. Lastly, Section 3.6 summarizes the methodology applied in this study.

### 3.2 Wind Farm System

In this section, the wind farm system based on the Park model is briefly described. The conventional Park model illustrates a static wake propagation, which means that it is unable to evaluate the practicality of real-time optimization. Hence, a delay structure is added to the Park model in illustrating the duration of wake propagation.

Park model is the most discussed wind farm model among the studies that had been previously conducted (Scholbrock, 2011) (Porté-Agel *et al.*, 2013). This model illustrates the expansion of the wake effect according to the distance between two wind turbines, and further classifies the wake effect by estimating the velocity profile of a single turbine, as shown in Figure 3.1 and Figure 3.2, respectively. However, the model does not illustrate the duration of a wake travelling from one wind turbine to the next. In order to evaluate the time efficiency of the optimization process, a delay structure was applied to the Park model (Gebraad *et al.*, 2013). Consequently, the time interval for the wake to travel from one wind turbine to another is considered in the wind farm system. Hence, the actual transition time of the wake effect can be determined.

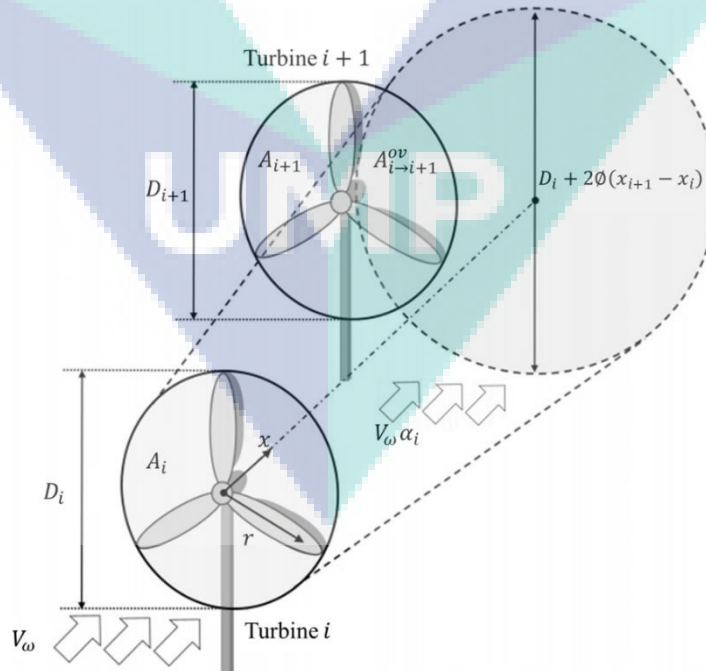


Figure 3.1 The expansion of wake in Park model

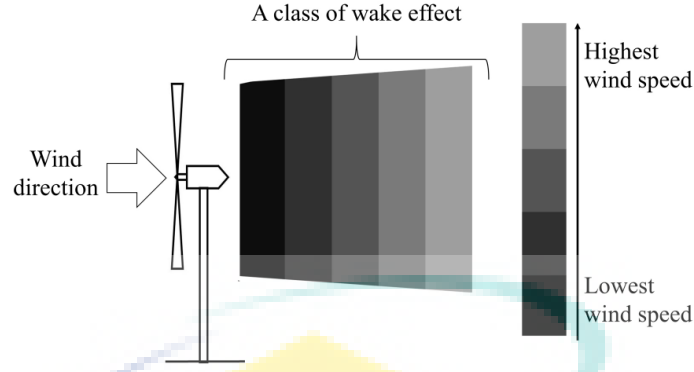


Figure 3.2 Classification of wake effect in Park model by estimating velocity profile of single turbine

Source: Churchfield (2013)

First, the static wake interaction between two wind turbines is briefly described according to Figure 3.1. Let  $X = \{1, 2, \dots, n\}$  be a set of  $n$  wind turbines in the wind farm.  $V_\omega$  is the incoming wind speed,  $\alpha_i$  and  $D_i$  are the axial induction factor and rotor diameter of the wind turbine  $i$ , respectively.  $A_{i+1}$  is the rotor swept area of the wind turbine,  $i + 1$ ,  $A_{i \rightarrow i+1}^{ov}$  is the overlapped area between the wake interaction generated by the upstream wind turbine  $i$  and downstream wind turbine  $i + 1$  and  $\emptyset$  is the roughness coefficient that represents the slope of wake expansion. If  $(x, r)$  is a point in the wake of the wind turbine, where  $x$  is the distance to the rotor disk plane of the turbine and  $r$  is the distance to the centerline of the wind turbine rotor axis; then, the aggregate wind velocity is given as:

$$\bar{V}_{i+1} = V_\omega (1 + \Delta \bar{V}_{i+1}), \quad 3.1$$

for

$$\Delta \bar{V}_{i+1} = \sqrt{\sum_{i \in X: x_i < x_{i+1}} \left( \alpha_i \left( \frac{A_{i \rightarrow i+1}^{ov}}{A_{i+1}} \right) \left( \frac{D_i}{D_i + 2\emptyset(x_{i+1} - x_i)} \right)^2 \right)^2}, \quad 3.2$$

where  $x_i$  and  $x_{i+1}$  are the distances to the rotor disk plane of the wind turbines  $i$  and  $i + 1$ , respectively. The wake interaction between the two turbines is illustrated in Figure 3.1. Noted that the aggregated wind velocity,  $V_{i+1}$  for  $(i + 1) \in X$  is evaluated based on the aggregation of the wind velocity deficit created by each upstream turbine. Furthermore, the diameter of the wake is assumed to have a circular cross-section and expands proportionally to the distance  $x$ . Then, the power production of each turbine can be represented as:

$$Q_i = 2\rho A_i \alpha_i (1 - \alpha_i)^2 \bar{V}_i^3, \quad 3.3$$

where  $\rho$  is the air density. Then, the total power production of the wind farm is the submission of  $Q_i$  ( $i = 1, 2, \dots, n$ ), which is given as:

$$\bar{Q}(\alpha_1, \alpha_2, \dots, \alpha_n) = \sum_{i=1}^n Q_i(\alpha_1, \alpha_2, \dots, \alpha_n). \quad 3.4$$

Next, the dynamics of the wake interaction is illustrated based on the estimation of the wake travel time from one turbine to another, as studied in Gebraad *et al.* (2013). Let  $\tau(i)$  be the index of the nearest neighbour downstream turbine of turbine  $i$ , where it is directly influenced by turbine  $i$ . Let also  $\lambda(i) = \{i, \tau(i), \tau(\tau(i)), \dots\}$  be the set that includes turbine  $i$  and the other downstream turbines in a row that is affected by turbine  $i$ . Then, the time interval  $T_\omega$  for the wake to travel to the whole wind farm can be approximated as:

$$T_\omega \approx \max_{i \in X} \left( \sum_{(i+1) \in \lambda(i)} \frac{x_{\tau(i)} - x_{i+1}}{\frac{1}{2}(\bar{V}_{i+1}(1 - 2\alpha_{i+1}) + \bar{V}_{\tau(i+1)})} \right). \quad 3.5$$

**Remark 3.1:** Please note that the Multi-Resolution Optimize Relative Step Size Random Search (MR-ORSSRS) based method optimizes the wind farm based on the inputs and outputs information as shown in Figure 3.3, where the inputs are the incoming wind speed  $V_\omega$  and axial induction factor  $\alpha_i$  ( $i = 1, 2, \dots, n$ ) while the output is the total power production  $\bar{Q}(\alpha_1, \alpha_2, \dots, \alpha_n)$ . The wind farm system is only applied for performance evaluation, where the relation between  $V_\omega$ ,  $\alpha_i$  ( $i = 1, 2, \dots, n$ ) and  $\bar{Q}(\alpha_1, \alpha_2, \dots, \alpha_n)$  remains unknown.

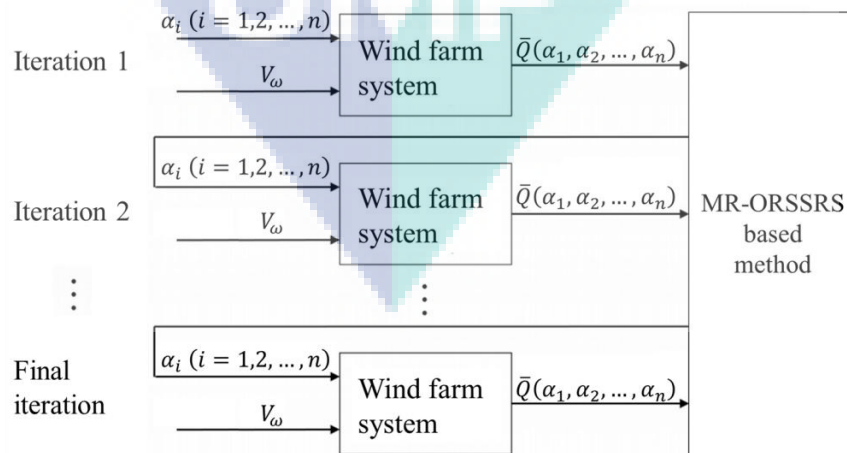


Figure 3.3 Model-free approach optimization of MR-ORSSRS based method

### 3.3 Problem Formulation

Considering a wind farm system in Section 3.2 consisting of  $n$  turbines, which are randomly placed in a location, and wind speed  $V_\omega$  is occurring in an arbitrarily direction. Meanwhile, the control parameter of each wind turbine is  $\alpha_i$ , where ( $i = 1, 2, \dots, n$ ) is the number of wind turbines and the power production of the wind turbine  $i$  is  $\bar{Q}(\alpha_1, \alpha_2, \dots, \alpha_n)$ . Here,  $\alpha_i$  is the corresponding axial induction factor of the wind turbine  $i$  which is generalized from the control parameters such as the blade pitch angle and the wind turbine yaw angle (Bianchi *et al.*, 2011). Following this, this study is executed based on a dynamic wind model, which means that the variations of wind speed and direction are included in the investigation of the real-time optimization performance. Therefore, it is expected that the power production of wind turbine  $i$ ,  $Q_i$  is not only relying on the control parameter of itself,  $\alpha_i$  but also affected by the control parameters of the other wind turbines,  $\alpha_1, \alpha_2, \dots, \alpha_{i-1}, \alpha_{i+1}, \dots, \alpha_n$  due to the interaction of the wake among the wind turbines. Similarly, the control parameter of turbine  $i$ ,  $\alpha_i$  is not only affecting the changes in the power production of itself, which is the  $Q_i$  but also affecting the changes in the power production of the other wind turbines,  $Q_1, Q_2, \dots, Q_{i-1}, Q_{i+1}, \dots, Q_n$ . Consequently,  $Q_i$  is directly affected by  $\alpha_i$  and indirectly affected by  $\alpha_1, \alpha_2, \dots, \alpha_{i-1}, \alpha_{i+1}, \dots, \alpha_n$ . Hence, the relations between  $Q_i$  and  $\alpha_1, \alpha_2, \dots, \alpha_n$  is difficult to be accurately modeled due to the complexity of the wake dynamic, which interacts between the wind turbines throughout the wind farm, as shown in Figure 3.4.

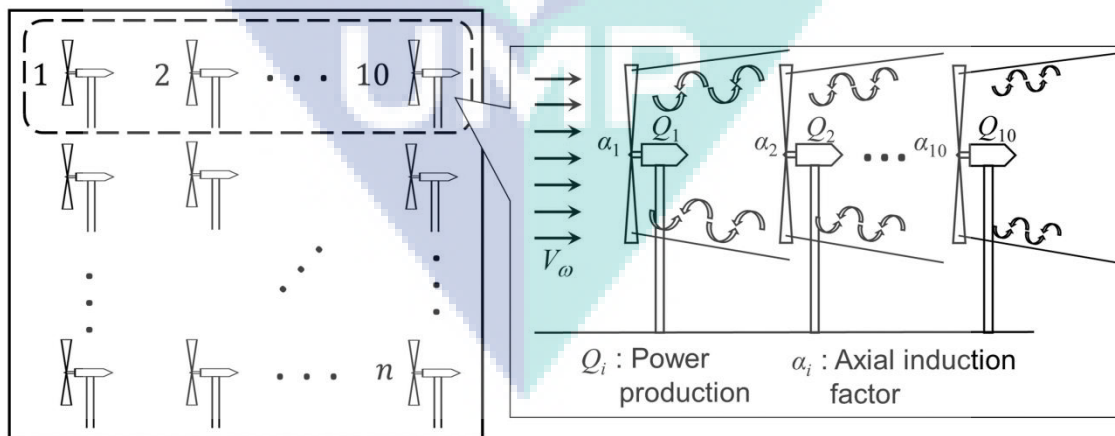


Figure 3.4 Illustration of wake aerodynamic interaction between wind turbines in wind farm.

Nevertheless, the optimization problem is described as follow:

**Problem 3.1:** Find axial induction factors  $(\alpha_1, \alpha_2, \dots, \alpha_n)$  to maximize the total power production  $\bar{Q}(\alpha_1, \alpha_2, \dots, \alpha_n)$ , while the exact formulation of  $Q_i(\alpha_1, \alpha_2, \dots, \alpha_n)$  remains unknown.

### 3.4 Random Search Based Optimization Methods

This section presents the method to solve Problem 3.1. Firstly, the operation of the standard ORSSRS is briefly reviewed. Then, the MR-ORSSRS is proposed as a new method to solve the problem in the standard ORSSRS algorithm.

#### 3.4.1 Optimized Relative Step Size Random Search

Random Search (RS) based method is a non-gradient optimization algorithm to optimize the design parameters according to the fitness of the objective function, which presents suitability for a model-free optimization. With this, the essential feature of RS-based algorithm is to store the best objective function for the fitness evaluation in every iteration. Hence, RS-based algorithm such as ORSSRS can provide a more stable objective function.

Next, the fundamental operation of ORSSRS is explained as follows. Let the optimization problem, given by:

$$\max_{\vartheta \in \mathbb{R}^N} F(\vartheta), \quad 3.6$$

where  $F: \mathbb{R}^N \rightarrow \mathbb{R}$  is the objective function and  $\vartheta \in \mathbb{R}^N$  is the design parameter.

The ORSSRS updates the design parameter,  $\vartheta$  by performing hypersphere neighborhood search as follows:

$$\vartheta(t) = \vartheta(t-1) - \beta(t), \quad 3.7$$

where  $\beta(t)$  is the updated sequence with relative to the step size of  $t^{\text{th}}$  iteration ( $t = 0, 1, \dots$ ) and it is given as:

$$\beta(t) = R(t)S e^{(t+1)\delta}. \quad 3.8$$

Here,  $\beta(t)$  is decreasing exponentially as the number of iteration  $t$  increases,  $e^{(t+1)\delta}$  is the exponent gain and  $\delta$  is a negative constant ( $\delta < 0$ ). Next, the symbol  $S$  is the step

size constant and  $R(t)$  is the  $N$ -dimensional random vector given in the element-wise Bernoulli distribution:

$$\begin{cases} \mathbb{P}(R(t) = -1) = 0.5, \\ \mathbb{P}(R(t) = 1) = 0.5. \end{cases} \quad 3.9$$

Next, the operation of the standard ORSSRS is described in Algorithm 3.1.

**Algorithm 3.1:** Standard ORSSRS algorithm.

---

Determine constant coefficients  $S$  and  $\delta$  for update sequence  $\beta(t)$  in Equation 3.8, set  $t = 0$  and initialize  $\vartheta(0)$  randomly.

Step (1) Initiate optimum design parameter and objective function

$$\begin{aligned} \vartheta^* &= \vartheta(0) \\ F^* &= F(\vartheta(0)) \end{aligned}$$

Step (2) Calculate hypersphere design parameters

$$\begin{aligned} \vartheta(t) &= \vartheta(t-1) - \beta(t) \\ &\text{where } \beta(t) \text{ and } R(t) \text{ are from Equation 3.8 and 3.9, respectively.} \end{aligned}$$

Step (3) Update the optimum design parameters and objective function

$$\begin{aligned} \mathbf{if } F(\vartheta(t)) > F^* \mathbf{ then} \\ \vartheta^* &\equiv \vartheta(t) \\ F^* &\equiv F(\vartheta(t)) \end{aligned}$$

**else**  
remain  $\vartheta^*$  and  $F^*$

**end if**

Step (4) Check the termination criterion

**if**  $t$  fulfills termination **then**  
algorithm ends with an optimum solution

$$\vartheta^* \equiv \arg \max_{\vartheta \in (\vartheta(0), \vartheta(1), \dots, \vartheta(t+1))} F(\vartheta)$$

**else**

set  $t = t + 1$  and repeat Step (2) to Step (4)

**end if**

---

In general, a standard ORSSRS can solve the high-dimensional optimization problem. Nevertheless, the ORSSRS does not have the capability of a real-time optimization due to an insufficient convergence rate. This is because the number of



evaluation needed to achieve successful convergence is proportional to the dimension of design parameter (Spall *et al.*, 1999).

In order to verify this statement, consider the optimization of the objective function as:

$$F(\vartheta) = ((\vartheta - 1)^\top (\vartheta - 1)), \quad 3.10$$

where  $\vartheta = [\vartheta_1, \vartheta_2, \dots, \vartheta_N]^\top$  and  $F(\vartheta^*) = 0$  at  $\vartheta^* = [1, 1, \dots, 1]^\top$  and the termination criterion is:

$$|F(\vartheta(t+1)) - F(\vartheta(t))| < \varepsilon, \quad 3.11$$

where  $\varepsilon$  is a small number  $\varepsilon = 0.01$ . Then, convergence time required to optimize the problem consisting of the number of dimensions  $N = (10, 50, 100, 500, 1000)$  as shown in Table 3.1. It evidently shows that the larger number of design parameters require a longer convergence time.

Table 3.1 The required convergence time for different sizes of dimension

Dimension number $N$	10	50	100	500	1000
Convergence time (s)	0.201	1.563	10.873	150.673	532.276

Moreover, the application of wind farm is also included to verify shall larger number of wind turbines would cause a longer optimization convergence time. Problem 3.1 is considered as the optimization problem in this case. Here, the objective function  $\bar{Q}$  and design parameters  $\alpha$  of Equation 3.4 are applied to  $F$  and  $\vartheta$  of Equation 3.6, respectively. Let the termination criterion of step (4) in Algorithm 3.1 be as the Equation 3.11. The convergence time required to optimize the wind farm consisting of different numbers of wind turbine  $n = (16, 32, 48, 64, 80)$  as shown in Table 3.2. It is expected that the convergence time increases proportionally to the number of wind turbines  $n$ .

Table 3.2 The required convergence time for different number of wind turbines

Number of wind turbines	16	32	48	64	80
Convergence time (hours)	46.732	116.056	150.209	196.517	222.308

In the case of maximizing the total power of wind farm, the application of a standard ORSSRS is still not capable of producing an acceptable convergence rate. For example, in the case of the Horns Rev wind farm in Denmark that has 80 wind turbines, the standard ORSSRS requires more than 200 hours to maximize the total power and it will be discussed in detail in Chapter 4. It shows that the high dimensional design parameter searching in the standard ORSSRS may not be a good solution from this problem. Therefore, the Multi-Resolution Optimize Relative Step Size Random Search (MR-ORSSRS) is introduced, which it is expected to produce a considerably better convergence rate, while maximizing the total power production.

### 3.4.2 Multi-Resolution Optimize Relative Step Size Random Search

Herewith, Equation 3.6 as the optimization problem is reconsidered. The new MR-ORSSRS is developed based on the standard ORSSRS to solve the problem. Unlike the standard ORSSRS, the optimization process of MR-ORSSRS is distributed to several stages consisting of different sizes of design parameter clusters (Ahmad *et al.*, August 2014). The details of the formulation is explained as follows:-

Consider the output of standard ORSSRS in Algorithm 3.1 as  $ORSSRS_{\vartheta}(F(\vartheta), \vartheta(0), S, \delta)$ . Let  $m$  be the resolution step and it is a positive whole number, while  $G(j)$  ( $j = 1, 2, \dots, m$ ) is a series of the design parameter's groups which satisfies  $G(1) < G(2) < \dots < G(m)$ . Supposed that function  $\gamma_j: \mathbb{R}^{G(j)} \rightarrow \mathbb{R}^N$  ( $j = 1, 2, \dots, m$ ) is given. The termination criterion in Step (4) of Algorithm 3.1 is  $|F(\gamma_j(t+1)) - F(\gamma_j(t))| < \varepsilon$ , where  $\varepsilon$  is a small constant value. Then, the algorithm of MR-ORSSRS is given by:

$$\varphi_j^* = ORSSRS_{\varphi_j}(F(\gamma_j(\varphi_j)), \varphi_j(0), S_j, \delta_j) \quad 3.12$$

for  $j = 1, 2, \dots, m$ .

Here,  $\varphi_1(0)$  is randomly initialized and  $\varphi_j(0)$  is a vector which satisfies  $\gamma_j(\varphi_j) = \gamma_{j-1}(\varphi_{j-1}^*)$  for  $j = 1, 2, \dots, m$ . Meanwhile,  $\varphi_m^*$  is denoted as the optimal output of MR-ORSSRS.

Next, the operation of MR-ORSSRS is demonstrated in a simple illustration.  $\vartheta \in \mathbb{R}^9$  is represented by the grey colored cross symbols as shown in Figure 3.5. The MR-ORSSRS is going to maximize  $F(\vartheta)$  for  $m = 3$ . Noted that, the groups of design parameters in the same dashed-box have the same value. Thus, the solution of the problem for each resolution is described as follows:

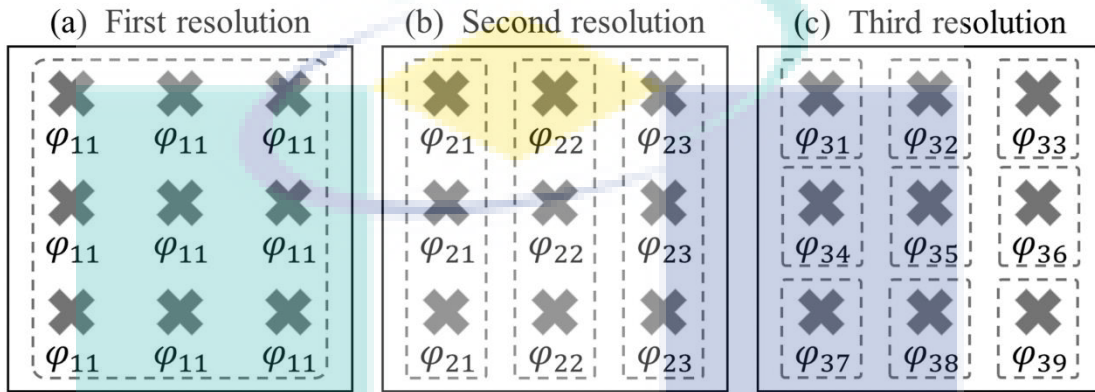


Figure 3.5 The illustration of MR-ORSSRS with three resolution step,  $m = 3$  and the grey colored crosses are the design parameters,  $\vartheta \in \mathbb{R}^9$ .

I. First resolution,  $j = 1$

$$\varphi_1^* = ORSSRS_{\varphi_1}(F(\gamma_1(\varphi_1)), \varphi_1(0), S_1, \delta_1) \quad 3.13$$

Figure 3.5(a) is the illustration of the first resolution.  $S_1$  and  $\delta_1$  are the constant coefficients for Equation 3.12 of  $j = 1$ . Here, the objective functions are clustered as one group such that  $G(1) = 1$ ; thus,  $\varphi_1 = \varphi_{11} \in \mathbb{R}$  for  $\gamma_1(\varphi_1) = [\varphi_{11} \varphi_{11} \dots \varphi_{11}] \in \mathbb{R}^9$ . Whereas,  $\varphi_1(0)$  is the random initial condition.

II. Second resolution,  $j = 2$

$$\varphi_2^* = ORSSRS_{\varphi_2}(F(\gamma_2(\varphi_2)), \varphi_2(0), S_2, \delta_2) \quad 3.14$$

Figure 3.5(b) is the illustration of the second resolution.  $S_2$  and  $\delta_2$  are the constant coefficients for Equation 3.12 of  $j = 2$ . Here, the objective functions are clustered as three groups such that,  $G(2) = 3$ ; thus,  $\varphi_2 = [\varphi_{21} \varphi_{22} \varphi_{23}] \in \mathbb{R}^3$  for  $\gamma_2(\varphi_2) = [\varphi_{21} \varphi_{21} \varphi_{21} \varphi_{22} \varphi_{22} \varphi_{22} \varphi_{23} \varphi_{23} \varphi_{23}] \in \mathbb{R}^9$ . Meanwhile,  $\varphi_2(0) = [\varphi_{11}^* \varphi_{11}^* \varphi_{11}^*]$ .

III. Third resolution,  $j = 3$

$$\varphi_3^* = ORSSRS_{\varphi_3}(F(\gamma_3(\varphi_3)), \varphi_3(0), S_3, \delta_3) \quad 3.15$$

Figure 3.5(c) is the illustration of the second resolution.  $S_3$  and  $\delta_3$  are the constant coefficients for Equation 3.12 of  $j = 3$ . Here, the objective functions are in stand-alone group such that,  $G(3) = 9$ ; thus,  $\varphi_3 = [\varphi_{31} \varphi_{32} \dots \varphi_{39}] \in \mathbb{R}^9$  for  $\gamma_3(\varphi_3) = [\varphi_{31} \varphi_{34} \varphi_{37} \varphi_{32} \varphi_{35} \varphi_{38} \varphi_{33} \varphi_{36} \varphi_{39}] \in \mathbb{R}^9$ . Whereas,  $\varphi_3(0) = [\varphi_{21}^* \varphi_{22}^* \varphi_{23}^* \varphi_{21}^* \varphi_{22}^* \varphi_{23}^* \varphi_{21}^* \varphi_{22}^* \varphi_{23}^*]$ . In the end of the resolution, the optimal solution  $\vartheta^* = \varphi_3^*$ .

Then, the procedure of the MR-ORSSRS is described in Algorithm 3.2

**Algorithm 3.2:** MR-ORSSRS algorithm.

---

Define the values for  $m, \varepsilon, G(j)$  ( $j = 1, 2, \dots, m$ ),  $\gamma_j$  ( $j = 1, 2, \dots, m$ ),  $S_j$  ( $j = 1, 2, \dots, m$ ) and  $\delta_j$  ( $j = 1, 2, \dots, m$ ). Initialize  $\varphi_1(0)$  and set  $j = 1$ .

Step (1) Acquire output of resolution

$$\varphi_j^* = ORSSRS_{\varphi_j}(F(\gamma_j(\varphi_j)), \varphi_j(0), S_j, \delta_j)$$

Step (2) Check termination of resolution

**if**  $|F(\varphi_j(t+1)) - F(\varphi_j(t))| \geq \varepsilon$  **then**

set  $t = t + 1$  and repeat Step (1) to (2)

**else**

Check the number of resolution

**if**  $j < m$  **then**

set  $j = j + 1$ ,  $\varphi_j(0) = \varphi_{j-1}^*$  and repeat Step (1)

**else**

Algorithm ends with the optimal solution,  $\vartheta^* = \varphi_j^*$

**end if**

**end if**

---

The operation of MR-ORSSRS algorithm is illustrated and described in Figure 3.5 and Algorithm 3.2, respectively. It is notable that MR-ORSSRS only works for a certain classes of problems which satisfies the condition such that a group of design parameters of the problem can have the same solution (Ahmad *et al.*, 2014). For example, in the optimization of the wind farm, wind turbines with the same number of upstream wind turbines will have the same solution. Therefore, MR-ORSSRS is suitable to optimize the wind farm problem.

### 3.5 Model-free Design for Wind Farm Total Power Production Maximization

The implementation of an MR-ORSSRS algorithm to solve Problem 3.1 is explained in this section. Here, the objective function,  $\bar{Q}$  and design parameters  $\alpha := (\alpha_1, \alpha_2, \dots, \alpha_n)$  of the wind farm from Equation 3.4 are applied to  $F$  and  $\vartheta$  of Equation 3.12, respectively. Hence, the implementation of MR-ORSSRS algorithm for the wind farm optimization is expressed as follow:

$$\varphi_j^* = \text{ORSSRS}_{\varphi_j} \left( \bar{Q} \left( \gamma_j(\varphi_j) \right), \varphi_j(0), S_j, \delta_j \right) \quad 3.16$$

for  $j = 1, 2, \dots, m$ . Then, refer to Algorithm 3.2, the implemented MR-ORSSRS algorithm for the wind farm optimization is presented in Algorithm 3.3.

**Algorithm 3.3:** Implementation of an MR-ORSSRS algorithm for a wind farm optimization.

---

Define the values for  $m, \varepsilon, G(j)$  ( $j = 1, 2, \dots, m$ ),  $\gamma_j$  ( $j = 1, 2, \dots, m$ ),  $S_j$  ( $j = 1, 2, \dots, m$ ) and  $\delta_j$  ( $j = 1, 2, \dots, m$ ). Initialize  $\varphi_1(0)$  and set  $j = 1$ .

Step (1) Acquire output of resolution

$$\varphi_j^* = \text{ORSSRS}_{\varphi_j} \left( \bar{Q} \left( \gamma_j(\varphi_j) \right), \varphi_j(0), S_j, \delta_j \right)$$

Step (2) Check termination of resolution

**if**  $\left| \bar{Q} \left( \varphi_j(t+1) \right) - \bar{Q} \left( \varphi_j(t) \right) \right| \geq \varepsilon$  **then**

set  $t = t + 1$  and repeat Step (1)

**else**

Check number of resolution

**if**  $j < m$  **then**

set  $j = j + 1$ ,  $\varphi_j(0) = \varphi_{j-1}^*$  and repeat Step (1)

**else**

MR-ORSSRS ends with optimal solution,  $\alpha^* = \varphi_j^*$

**end if**

**end if**

---

In the greedy control of the wind farm, the control parameters of wind turbines are set to the maximum, which produces the axial induction factor of  $1/3$  (Marden *et al.*, 2013). However, because of the wake dynamic, the axial induction factor is required to be reduced as a compensation between the wind turbines to obtain maximum power

production. Therefore, in this study, the axial induction factor of the wind turbines is set to a maximum before the optimization starts. Hence, at the beginning of the optimization,  $\varphi_1(0)$  is set to  $1/3$ .

According to Algorithm 3.3, the value of  $m$ ,  $G(j)$  ( $j = 1, 2, \dots, m$ ) and  $\gamma_j$  ( $j = 1, 2, \dots, m$ ) can significantly affect the optimization performance. Meanwhile, these values are considered based on the conditions of wind farm layout, wind direction and group strategy. For example,  $m$  is the maximum number of resolution with the reasonable value set between 3 to 5. This is because a bigger value of  $m$  will prolong the optimization computation time, while having insignificant improvement to the power production (Ahmad *et al.*, August 2014). Since most of the existing wind farm layouts are symmetrically distributed such that the distance between the rows and columns are identical,  $3 \leq m \leq 5$  is preferable in this study due to the time constraints for computation. In the meantime,  $\gamma_j$  and  $G(j)$  are the group strategy and number of group at the resolution  $j$ , respectively, with  $j = 1, 2, \dots, m$ . On this note, the strategy of grouping in MR-ORSSRS is based on the design parameters, where they have similar optimum output.

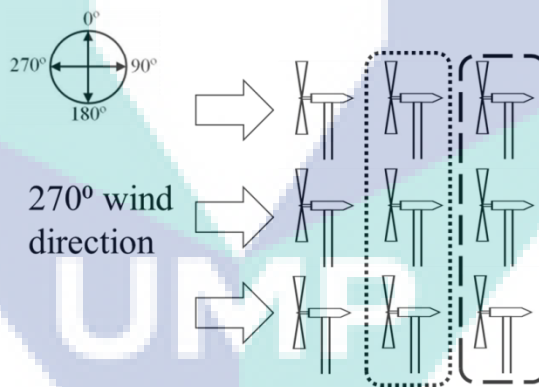


Figure 3.6 Wind farm consists 9 wind turbines wind direction at 270°.

For example, Figure 3.6 shows a wind farm with 9 wind turbines and the wind is occurring at the direction of 270°. The wind turbines covered by a dash-line are at the last row, while the wind turbines covered by the dotted-line are in the middle row. Here, the wind turbines in the last row do not have any other downstream wind turbines. Without the need to further tolerate with any downstream wind turbines due to the wake effects, these turbines are able to extract wind power at a maximum rate. Thus, they have the same axial induction factor at a maximum,  $\alpha = 1/3$ . On the other hand, the wind

turbines covered with the dotted-lines have a downstream wind turbine for each of them. Following similar perspective, their axial induction factor would definitely be less than  $1 / 3$  while having the similar axial induction factors, as they are required to only tolerate for one downstream wind turbine. Consequently, the grouping strategy of wind turbines can be decided base on the number of downstream wind turbines.

Next, the detail explanation of grouping strategy is discussed in Table 3.3.

Table 3.3 Group strategy with the corresponded resolution,  $j$ .

Resolution	Strategy
$j = 1$	2 groups are formed, $G(1) = 2$ . The wind turbines which have downstream wind turbines are merged in a group, $g_{11}$ . Meanwhile, the wind turbines without downstream wind turbines are grouped in another group, $g_{12}$ . With this, the turbines in $g_{12}$ are set to maximum induction factor, $\alpha = 1 / 3$ as they do not have to tolerate with wake interaction.
$2 \leq j < m$	$g_{11}$ is divided into several groups according to the number of corresponded downstream wind turbines, while the group $g_{12}$ is remained as the previous resolution.
$j = m$	In the last resolution, each group consists of a standalone wind turbine such that $G(m) = n$ , where $n$ is the maximum number of wind turbines in the wind farm.

Next, an example on the implementation of MR-ORSSRS to optimize a wind farm with 16 wind turbines is demonstrated. Considering the wind farm layout in Figure 3.7; the wind is occurring at the direction of  $225^\circ$ . Here, the objective is to find the optimal axial induction factor  $\alpha_i$  ( $i = 1, 2, \dots, 16$ ) in order to maximize the total power production  $\bar{Q}(\alpha_1, \alpha_2, \dots, \alpha_{16})$ . The number of resolution  $m = 3$  is selected for this case.

First, there are two groups of wind turbines,  $G(1) = 2$  in the first resolution,  $j = 1$  which are  $\varphi_1$  and  $\varphi_2$ . Meanwhile, the corresponding wind turbines in each group are  $g_{11} = (5, 6, 7, 9, 10, 11, 13, 14, 15)$  and  $g_{12} = (1, 2, 3, 4, 8, 12, 16)$ , respectively. The group strategy is in accordance to  $j = 1$  as shown Table 3.3 and  $\gamma_1(G(1)) = [\varphi_{12}, \varphi_{12}, \varphi_{12}, \varphi_{12}, \varphi_{11}, \varphi_{11}, \varphi_{11}, \varphi_{12}, \varphi_{11}, \varphi_{11}, \varphi_{11}, \varphi_{12}, \varphi_{11}, \varphi_{11}, \varphi_{11}, \varphi_{12}]^T \in \mathbb{R}^{16}$ .

In the second resolution,  $j = 2$ , the wind turbines are distributed into four groups,  $G(2) = 4$ . Therefore, there are four parameters  $\varphi_1, \varphi_2, \varphi_3$  and  $\varphi_4$  that are required to be optimized. Meanwhile, the corresponding wind turbines in each group are  $g_{21} = (13)$ ,

$g_{22} = (9, 10, 14)$ ,  $g_{23} = (5, 6, 7, 11, 15)$  and  $g_{24} = (1, 2, 3, 4, 8, 12, 16)$ , respectively. Here, the grouping strategy is based on  $2 \leq j < m$  as shown in Table 3.3, where the wind turbines in  $g_{11}$  is divided into several smaller groups,  $g_{21}$ ,  $g_{22}$  and  $g_{23}$ , while the wind turbines in  $g_{12}$  remains in  $g_{24}$  and  $\gamma_2(G(2)) = [\varphi_{24}, \varphi_{24}, \varphi_{24}, \varphi_{24}, \varphi_{23}, \varphi_{23}, \varphi_{23}, \varphi_{24}, \varphi_{22}, \varphi_{22}, \varphi_{23}, \varphi_{24}, \varphi_{21}, \varphi_{22}, \varphi_{23}, \varphi_{24}]^T \in \mathbb{R}^{16}$ . The distribution is according to this structure because the 5<sup>th</sup>, 6<sup>th</sup>, 7<sup>th</sup>, 11<sup>th</sup> and 15<sup>th</sup> wind turbines have to contend solely with one downstream wind turbine at the same time, which means that they should have the same axial induction factor. Therefore, they are grouped in the same group  $g_{23}$ . However, the distribution is more adaptable in this stage, which can have more options such as  $g_{21} = (9, 10, 13, 14)$ ,  $g_{22} = (5, 6, 7, 11, 15)$  and  $g_{23} = (1, 2, 3, 4, 8, 12, 16)$  or  $g_{21} = (13)$ ,  $g_{22} = (5, 6, 7, 9, 10, 11, 14, 15)$  and  $g_{23} = (1, 2, 3, 4, 8, 12, 16)$ .

Lastly,  $j = m$  is the final resolution. According to the group strategy in Table 3.3, each wind turbine is distributed such that they are standalone,  $\varphi_i$  ( $i = 1, 2, \dots, 16$ ). Here,  $\gamma_3(G(3)) = [\varphi_{31}, \varphi_{32}, \dots, \varphi_{316}]^T \in \mathbb{R}^{16}$ .

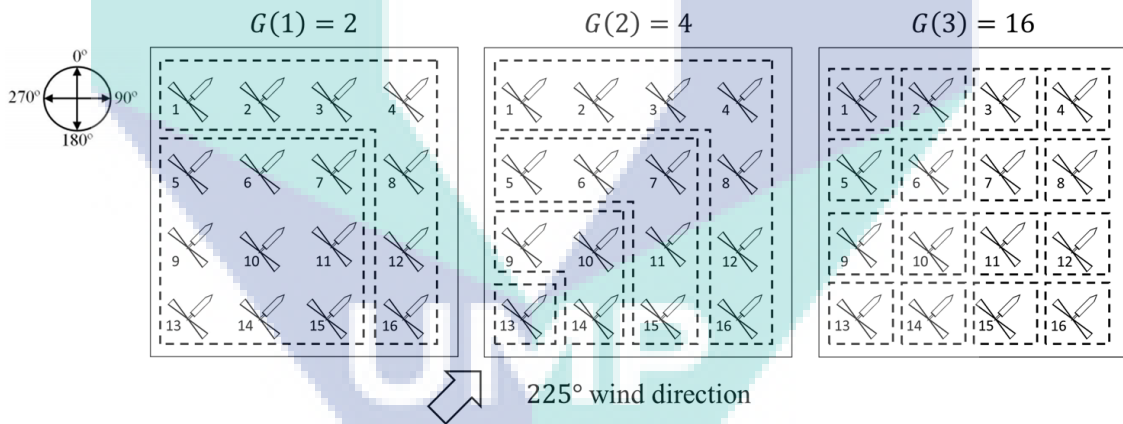


Figure 3.7 Wind farm layout of 16 wind turbines with incoming wind occurring at 225° direction.

### 3.6 Summary

The methodology to execute this study is discussed in this chapter. First, the wind farm system based on Park model is introduced. Park model is among the most studied wind farm models, as the representation of the wake effect provided in the Park model is simple and well-illustrated. It also includes the decay of the airspeed and expansion pattern of the wind (Scholbrock, 2011). However, the Park model is unable to provide a



practical evaluation of real-time optimization, because it is only representing a static wake interaction between the wind turbines. Therefore, a dynamic Park model is created by adding a delay structure to illustrate the duration required for the wake to travel from one wind turbine to the next wind turbines. Although the wind farm model is provided in this section, it is to emphasize that the model is only for evaluating the performance of the optimization algorithms. The optimization are carried out based on the information of inputs and outputs, while the relation between the inputs and outputs remains unknown.

Next, the wind farm problem is formulated. At this stage, the axial induction factor  $\alpha$  is assigned as the designed parameter, where the optimization algorithm is required to tune  $\alpha_i$  ( $i = 1, 2, \dots, n$ ) such that the total power production  $\bar{Q}$  is maximized. However, take note that  $\alpha_i$  is not the only contributing factor that will impact the power production of turbine  $i$   $Q_i$ . The existence of wake interaction has further complicated the relation between  $\alpha$  and  $\bar{Q}$ . In fact, it presents substantial effect on the power production of all downstream wind turbines which correspond with it. Hence, the relation between  $\alpha$  and  $\bar{Q}$  is formulated, as per Equation 3.4.

Furthermore, the step-by-step process of standard ORSSRS and MR-ORSSRS is presented. The generic features of the ORSSRS-based optimization algorithm include its ability to optimize large dimensional problems and its memorisable structure which allows a more stable objective function to achieved. However, the standard ORSSRS does not provide reasonable performance for real-time optimization, since its optimization convergence time is increasing proportionally to the size of problem dimension and the evidence is provided in Table 3.1 and Table 3.2. On the other hand, MR-ORSSRS solves the problem in convergence time by dividing a large dimensional optimization into several stages. In order to understand the processes for ORSSRS and MR-ORSSRS, the algorithm procedures are presented in Algorithm 3.1 and Algorithm 3.2, respectively. Furthermore, Algorithm 3.3 shows the implementation of Algorithm 3.2 for wind farm optimization. In totality, the group strategies of each resolution and the transition of designed parameters from one resolution to the next resolution are well-explained accompanied by some examples. The results, and discussion of the study will be presented in Chapter 4.

## CHAPTER 4

### RESULTS AND DISCUSSION

#### 4.1 Introduction

Performance of the Multi-Resolution Optimized Relative Step Size Random Search (MR-ORSSRS) based method is presented and discussed in this chapter. The presented results are obtained using a standard Optimize Relative Step Size Random Search (ORSSRS), Multi-Resolution Simultaneous Perturbation Stochastic Approximation (MR-SPSA) and MR-ORSSRS based methods in assessing the improvement and performance of the new MR-ORSSRS algorithm. Noted that the results of the MR-SPSA based method presented in this study are referred according to Ahmad *et al.* (2014).

In Section 4.2, the layout of the Horns Rev wind farm is briefly illustrated and discussed. A time interval for the wake to travel throughout the wind farm is included to illustrate the real situation in a wind farm. However, the time interval is different for each incoming wind direction. Hence, the formation of the time interval is discussed in detail. Each parameter of the Horns Rev wind farm is then summarized.

Next, the optimization performance on the wind farm's total power production is presented in Section 4.3. First, the algorithm parameters of the ORSSRS and MR-ORSSRS algorithms are given. Next, the results of the total power production according to the wind direction at  $170^\circ$ ,  $200^\circ$ ,  $220^\circ$ ,  $240^\circ$ ,  $250^\circ$  and  $270^\circ$  under static wind speed  $V_\omega = 8 \text{ m/s}$  are presented (Ahmad *et al.*, 2014). The total power production when the wind occurs at the directions of  $170^\circ$  and  $220^\circ$  is illustrated in order to observe the convergence patterns of the methods. Meanwhile, discussion on the group strategy for the first and second resolutions of the MR-ORSSRS is provided. The statistical analysis of all the directions is then summarized.

Following this, Section 4.4 presents a special case of wind turbine failure to evaluate the robustness of the MR-ORSSRS, MR-SPSA and ORSSRS methods in handling unpredictable events. Moreover, the experiment on non-static wind variation is included in Chapter 4.5, in order to validate the performance on real-time optimization by using the MR-ORSSRS, MR-SPSA and ORSSRS based methods. Lastly, Section 4.6 summarizes the results and discussion presented in this chapter.

## 4.2 Horns Rev Wind Farm

Horns Rev wind farm is located in Denmark. It is an offshore wind farm consisting of 80 (Vesta V80 2MW) wind turbines. A (Vesta V80 2MW) wind turbine has 80 m turbine diameter  $D$  and is able to produce the power up to 2 MW. Figure 4.1 shows the layout of the wind farm, which is in parallelogram. Each wind turbine is  $7 D$  away from each other, which is equivalent to 560 m in both the  $x$  and  $y$  directions. The roughness coefficient is  $\phi = 0.04$  and the air density is  $\rho = 1.225 \text{ kg} / \text{m}^3$ . Furthermore, the incoming wind direction at  $170^\circ, 200^\circ, 220^\circ, 240^\circ, 250^\circ$  and  $270^\circ$  are indicated by the red, orange, yellow, green, blue and purple dotted arrows, respectively. Table 4.1 summarizes the wind farm parameters.

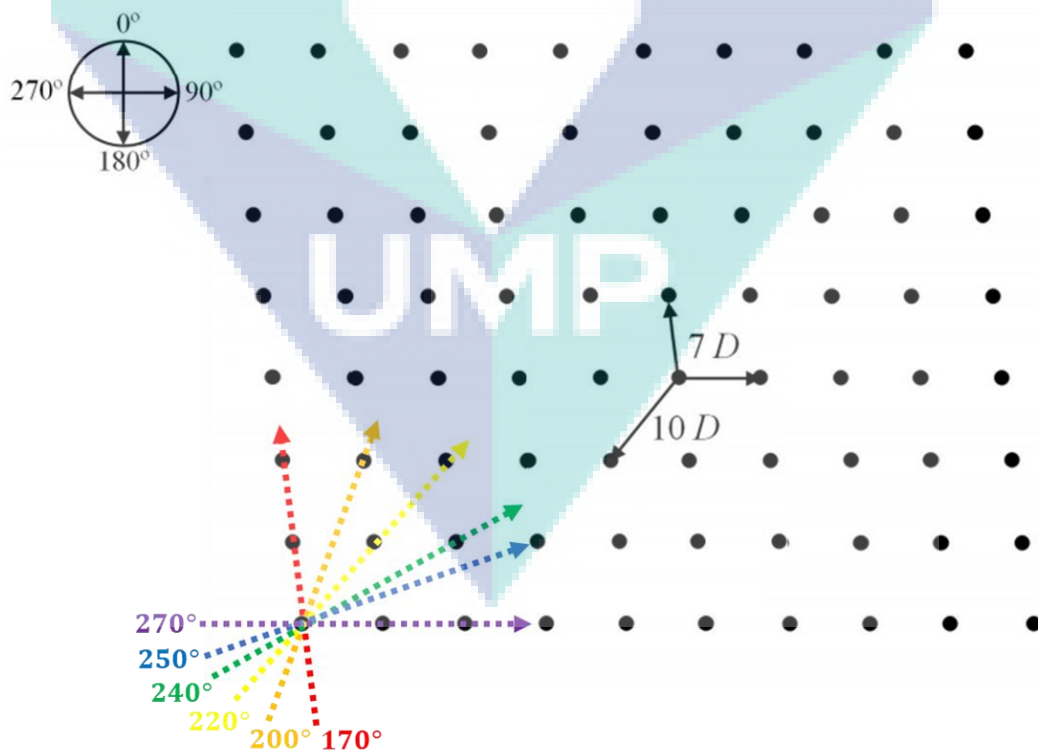


Figure 4.1 Horns Rev wind farm layout with incoming wind direction indicator.

Table 4.1 Wind farm parameters

Wind farm parameters	value					
Incoming wind direction	170°	200°	220°	240°	250°	270°
Air density $\rho$	1.225 kg/m <sup>3</sup>					
Number of wind turbine	80					
Roughness coefficient $\phi$	0.04					
Turbine diameter $D$	80 m					
Wind speed $V_\omega$	8 m/s					

In this case study, the wind speed is set to  $V_\omega = 8 \text{ m/s}$  (Ahmad *et al.*, 2014) and the incoming wind direction is suggested to occur at 170°, 200°, 220°, 240°, 250° and 270°. The axial induction factors of the 80 wind turbines are selected as design parameters,  $n = 80$ , and the time interval for the wake to travel throughout the wind farm  $T_\omega$  as mentioned in Equation 3.5 is different according to the wind direction - for example, in the case of 220°,  $T_\omega = 1400 \text{ s}$  and in the case of 240°,  $T_\omega = 1200 \text{ s}$ . This is because the number of wind turbine and distance between each wind turbine for the wake to travel thoroughly is different in each direction. Based on the fore-mentioned wind directions of 220° and 240°, the wake would travel through 7 and 4 wind turbines, while the distance for the wake to travel to the next wind turbine is  $10 D$  and  $15 D$ , as shown in Figure 4.2 and Figure 4.3, respectively. Herewith, Table 4.2 summarizes the time interval  $T_\omega$  for the wake to travel throughout the wind farm with incoming wind directions at 170°, 200°, 220°, 240°, 250° and 270°.

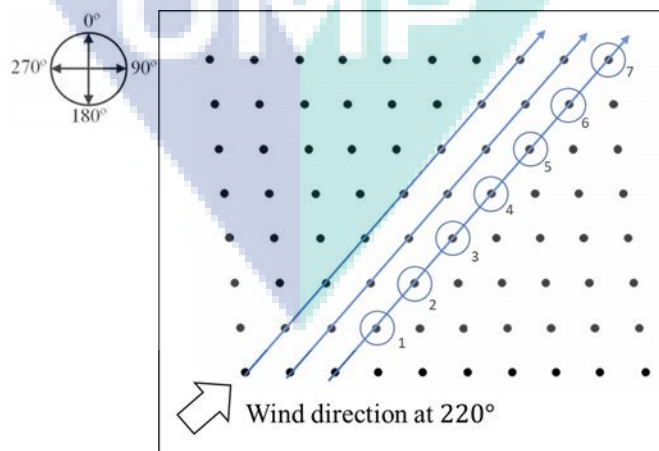


Figure 4.2 The number of wind turbines for the wake to travel through when the wind direction is at 220°.

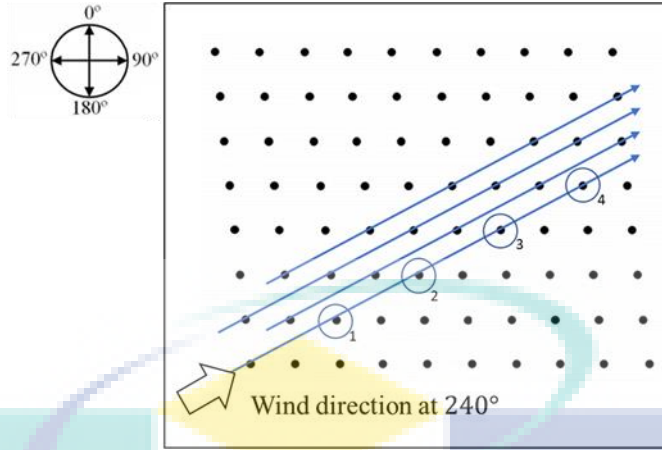


Figure 4.3 The number of wind turbine for the wake to travel through when wind direction occurs at 240°.

Table 4.2 Time interval  $T_\omega$  for wake to travel throughout wind farm

Wind farm parameters	value					
Wind direction	170°	200°	220°	240°	250°	270°
Time interval of wake $T_\omega$	980 s	900 s	1400 s	1200 s	1260 s	1260 s

### 4.3 The Performance of methods with Different Wind Direction

The algorithm parameters of ORSSRS and MR-ORSSRS algorithms must be initially defined, in order to perform the optimization of the wind farm total power production using ORSSRS and MR-ORSSRS based methods.

The step size and negative constant of Algorithm 3.1 is set to  $S = 0.04$  and  $\delta = -0.003$ , respectively. Note that the performance comparisons carried out in this study are limited to 700 hours of simulation time. Therefore, the termination criterion  $t_{max}$  of Algorithm 3.1 (ORSSRS) is different in each case of incoming wind direction, where  $t_{max}$  is the maximum number of iterations. For example,  $t_{max} = 2571$  for the incoming wind direction of 170°, with the time interval for the wake to travel throughout the wind farm at  $T_\omega = 980$  s, as according to Equation 3.5. On the other hand, when the incoming wind direction is now at 200°, the time interval for the wake to travel throughout the wind farm is  $T_\omega = 900$  s. Then, the termination criterion in this case is  $t_{max} = 2800$ . Table 4.3 summarizes the termination criterion  $t_{max}$  of Algorithm 3.1 for the incoming wind directions of 170°, 200°, 220°, 240°, 250° and 270°. Here, the formulation of the termination criterion  $t_{max}$  for Algorithm 3.1 is given as:

$$t_{max} = \frac{700 \times 3600}{T_{\omega}} \quad 4.1$$

Table 4.3 Parameters for Algorithm 3.1 (ORSSRS) for wind direction at 170°

Wind farm parameters	value					
Wind direction	170°	200°	220°	240°	250°	270°
Termination criterion $t_{max}$	2571	2800	1800	2100	2000	2000

Next, Table 4.4 presents the parameter of Algorithm 3.3. The maximum number of resolution and termination criterion are set to  $m = 3$  ( $j = 1, 2, 3$ ) and  $\varepsilon = 0.01$ , respectively. Meanwhile, the step size  $S_j$  and negative constant  $\delta_j$  for each resolution  $j = 1, 2, 3$  are summarized in Table 4.4.

Table 4.4 Parameters for Algorithm 3.3 (MR-ORSSRS)

Parameters	Value		
Maximum resolution	$m = 3$		
Termination criterion	$\varepsilon = 0.01$		
Step size	$S_1 = 0.085$	$S_2 = 0.0085$	$S_3 = 0.0028$
Negative constant	$\delta_1 = -0.095$	$\delta_2 = -0.023$	$\delta_3 = -0.003$

The algorithm parameters of MR-ORSSRS must be reconsidered because the wind farm configuration is different for each of the cases. Eventually, in this study, the value of step size  $S_j$  and negative constant  $\delta_j$  for all resolution  $j = 1, 2, \dots$  are carefully tuned by trial and error. Besides, one of the objectives is to evaluate the robustness of the MR-ORSSRS based method. Therefore, the parameters in Algorithm 3.3 are remained similar for all cases of wind direction as shown in Table 4.4. Nevertheless, the group selection of the first resolution and second resolution is different in each case of wind directions. Eventually,  $\gamma_j$  ( $j = 1, 2$ ) is different for each wind direction; yet, the function  $\gamma_j$  ( $j = m$ ) is similar for all wind directions as according to the grouping strategy in Section 3.5. In particular, the group number for the second resolution  $G(2)$  is sensitive to the variation in wind direction. For example, Figure 4.4 and Figure 4.5 show the group strategy of the first and second resolutions for the wind direction at 170°, respectively. Meanwhile, the group strategy for the first and second resolutions for the wind direction at 200° are

shown in Figure 4.6 and Figure 4.7, respectively. Based on the illustrations, it is clearly noted that group number of the second resolution  $G(2)$  is changing due to the variations in the incoming wind direction. Meanwhile, the group number in the first and last resolutions are  $G(1) = 2$  and  $G(3) = 80$ , respectively for all the incoming wind directions. With this, the group numbers of the second resolution  $G(2)$  for the wind direction of  $170^\circ$ ,  $200^\circ$ ,  $220^\circ$ ,  $240^\circ$ ,  $250^\circ$  and  $270^\circ$  are presented in Table 4.5.

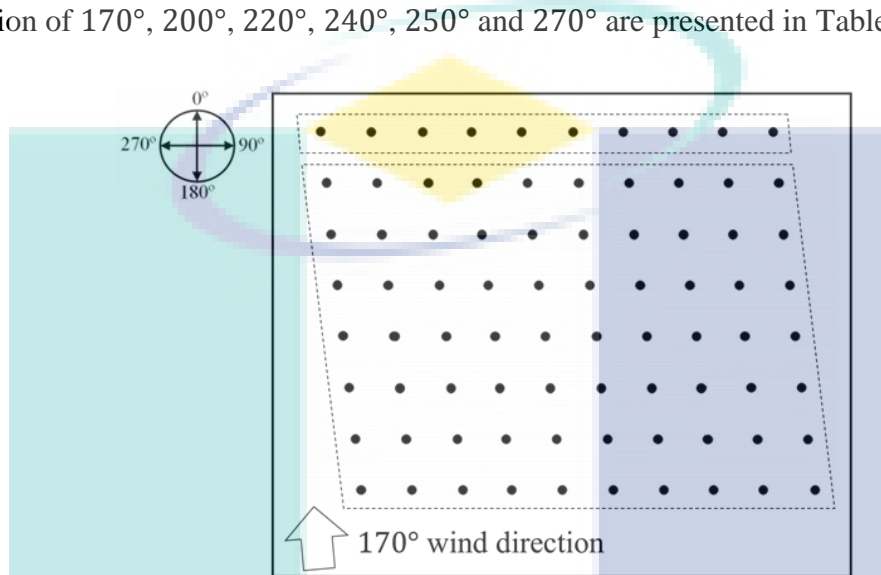


Figure 4.4 Group selection in the first resolution for the wind direction of  $170^\circ$ .

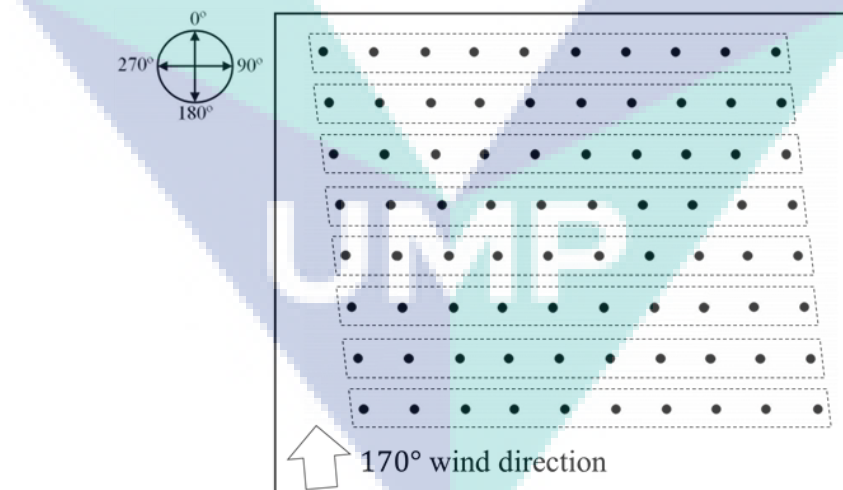


Figure 4.5 Group selection in the second resolution for the wind direction of  $170^\circ$ .

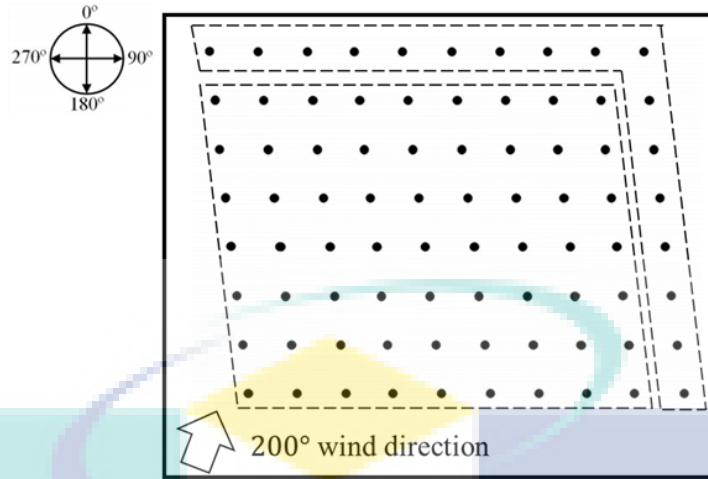


Figure 4.6 Group selection in the first resolution for the wind direction of 200°.

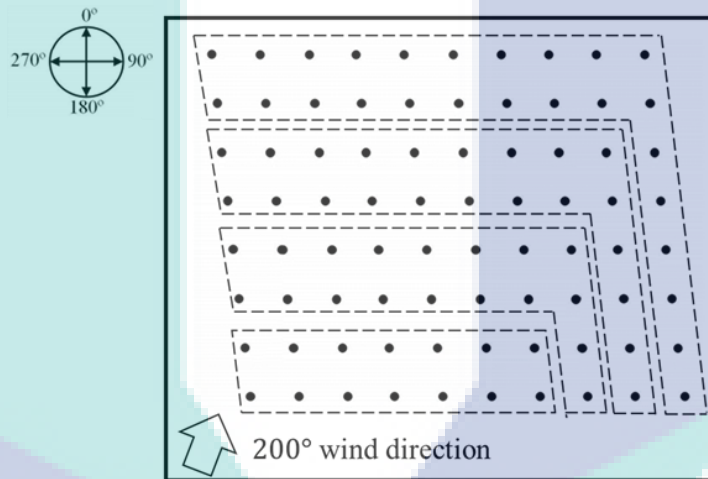


Figure 4.7 Group selection in the second resolution for the wind direction of 200°.

Table 4.5 Group number of the second resolution  $G(2)$  for Algorithm 3.3 (MR-ORSSRS).

Wind farm parameters	Value					
Wind direction	170°	200°	220°	240°	250°	270°
$G(2)$	8	4	8	5	4	10

In the following, findings on the total power production optimized using the MR-ORSSRS, MR-SPSA and ORSSRS based methods are presented. Figure 4.8 and Figure 4.9 present the results of the total power production  $\bar{Q}(\alpha_1, \alpha_2, \dots, \alpha_{80})$  of each method when wind occurs in the directions of 170° and 200°, respectively for the first 10 hours of simulation time. Meanwhile, Figure 4.10 and Figure 4.11 illustrate the results for 700



hours of simulation time. Here, the results of the MR-ORSSRS, MR-SPSA and ORSSRS based methods are represented by the blue line, green line and red line, respectively. The presented results are obtained after 100 trials due to the stochastic nature of the algorithms. Basically, the total power production of the wind farm has been successfully improved using each method during the 700 hours simulation time.

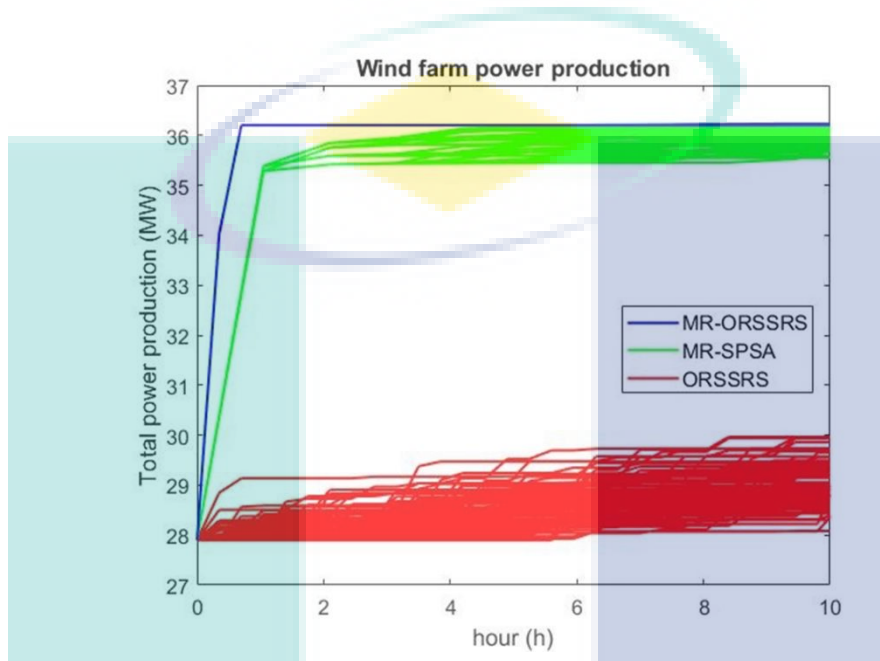


Figure 4.8 Results of the total power production  $\bar{Q}(\alpha_1, \alpha_2, \dots, \alpha_{80})$  during the first 10 hours of simulation time when wind occurs at the  $170^\circ$  direction

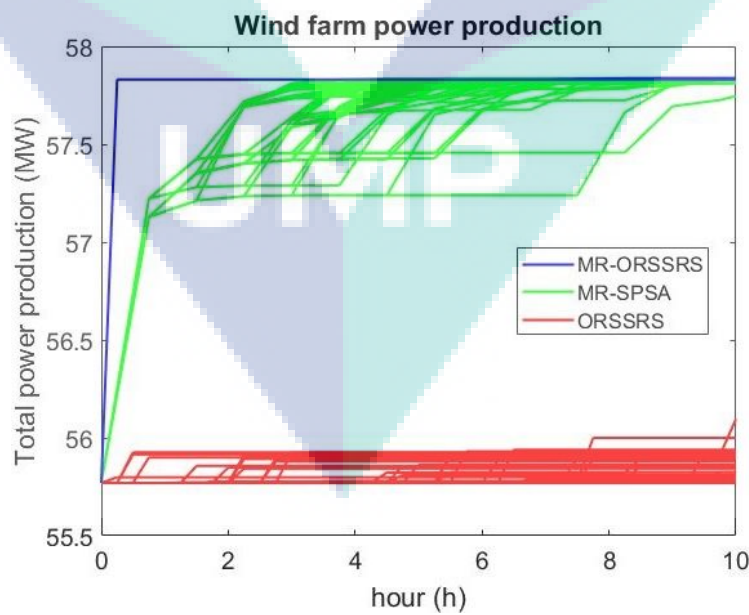


Figure 4.9 Results of the total power production  $\bar{Q}(\alpha_1, \alpha_2, \dots, \alpha_{80})$  in the first 10 hours of simulation time when wind occurs at the  $200^\circ$  direction.

Noticed that the MR-ORSSRS based method is leading the MR-SPSA and ORSSRS based methods for both the incoming wind directions at 170° and 200°, which shows that MR-ORSSRS has the shortest convergence time. Meanwhile, the MR-ORSSRS based method displays a tremendous convergence speed, and the convergence is precise for all the 100 trials such that all the lines merge into a single fine blue line as observed in Figure 4.8 and Figure 4.9. In general, the MR-ORSSRS based method has the highest total power production, which is comparable with the MR-SPSA based method; with the ORSSRS method producing the lowest total power production in the overall comparison, as shown in both Figure 4.10 and Figure 4.11.

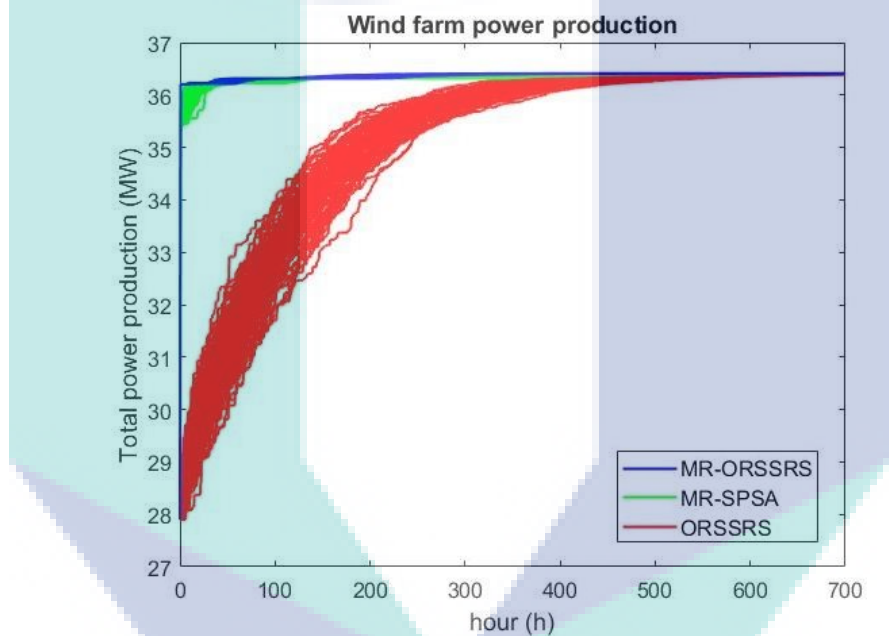


Figure 4.10 Results of full simulation time of total power production  $\bar{Q}(\alpha_1, \alpha_2, \dots, \alpha_{80})$  when wind is occurring at 170° direction.

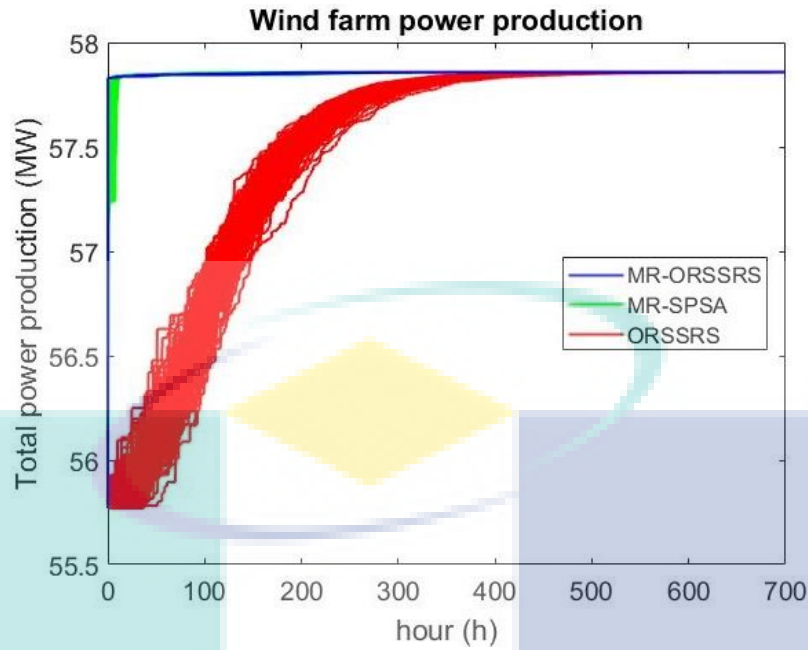


Figure 4.11 Results of the total power production  $\bar{Q}(\alpha_1, \alpha_2, \dots, \alpha_{80})$  during the full simulation time when the wind occurs at the  $200^\circ$  direction.

Moreover, the full statistical analysis on the total power production is recorded in Table 4.6. The findings indicate that MR-ORSSRS is able to produce the highest total power production, as compared to the MR-SPSA and ORSSRS based methods, where the maximum total power production yielded is  $63.693124 \text{ MW}$  when the wind direction is at  $250^\circ$ , as compared to  $63.6931204 \text{ MW}$  and  $63.692154 \text{ MW}$ , respectively. The MR-ORSSRS dominates the total power production in terms of mean, best, worst and standard deviations for the incoming wind direction of  $170^\circ, 200^\circ, 220^\circ$  and  $240^\circ$ . However, MR-ORSSRS based method produces less total power production in terms of the mean when the incoming wind directions occur at  $250^\circ$  and  $270^\circ$ , where the results obtained are  $63.6931077 \text{ MW}$  and  $38.1186700 \text{ MW}$ , as compared to the MR-SPSA based method which yields  $63.6931087 \text{ MW}$  and  $38.1186721 \text{ MW}$ , respectively. On the other hand, the MR-ORSSRS based method produces the lowest standard deviation of the total power production among the tested methods. With the overall standard deviation of the total power production as the basis, it shows that the MR-ORSSRS based method can produce higher consistency in total power production as compared to the MR-SPSA and ORSSRS based methods.

Furthermore, Table 4.7 shows the performance in convergence time through the MR-ORSSRS, MR-SPSA and ORSSRS based methods. The convergence time is defined as the time required to achieve 90% of the final value of the total power production during

the 700 hours. MR-ORSSRS based method has the fastest convergence time, where the shortest time is required to converge to 90% of the total power production, which is only 0.250 hours when incoming wind direction occurs at 200°; while the MR-SPSA and ORSSRS based methods each require 2.250 hours and 205.25 hours to achieve this value. Noted that the longest convergence time is required when the wind direction is at 220°. This is because the wind farm will experience a significantly greater wake effect when the wind comes from the direction of 220° (Porté-Agel *et al.*, 2013).

Table 4.6 Performance analysis of the total power production (MW) for MR-ORSSRS, MR-SPSA and ORSSRS with different wind directions. Std.: Standard deviation.

<b>Wind direction</b>		<b>ORSSRS</b>	<b>MR-SPSA</b>	<b>MR-ORSSRS</b>
170°	Mean	39.6020710	39.6055637	<b>39.6055672</b>
	Best	39.6052702	39.6055694	<b>39.6055768</b>
	Worst	39.5580275	39.6053917	<b>39.6054755</b>
	Std.	5378.131	17.625	<b>16.086</b>
200°	Mean	57.8580633	57.8581957	<b>57.8582120</b>
	Best	57.8581958	57.8582077	<b>57.8582177</b>
	Worst	57.8574196	57.8581800	<b>57.8581967</b>
	Std.	127.174	5.301	<b>4.583</b>
220°	Mean	48.2176232	48.2246182	<b>48.2253053</b>
	Best	48.2235997	48.2260427	<b>48.2264942</b>
	Worst	48.2012265	48.2193766	<b>48.2224691</b>
	Std.	4022.443	1128.643	<b>892.482</b>
240°	Mean	57.1768681	57.1787754	<b>57.1788215</b>
	Best	57.1782301	57.1788280	<b>57.1788466</b>
	Worst	57.1729688	57.1786632	<b>57.1787613</b>
	Std.	969.889	28.879	<b>17.541</b>
250°	Mean	63.6908652	<b>63.6931087</b>	63.6931077
	Best	63.6921514	63.6931204	<b>63.6931244</b>
	Worst	63.6881174	<b>63.6930852</b>	63.6930740
	Std.	942.328	<b>6.931</b>	9.414
270°	Mean	38.0984522	<b>38.1187021</b>	38.1186700
	Best	38.1155485	38.1187237	<b>38.1187321</b>
	Worst	37.8723097	38.1170564	<b>38.1182603</b>
	Std.	$346.364 \times 10^2$	166.404	<b>94.426</b>

Table 4.7 Performance analysis of the convergence time (h) for MR-ORSSRS, MR-SPSA and ORSSRS with different wind directions.

<b>Wind direction</b>		<b>ORSSRS</b>	<b>MR-SPSA</b>	<b>MR-ORSSRS</b>
170°	Mean	199.193	11.376	<b>0.544</b>
	Best	149.450	4.900	<b>0.544</b>
	Worst	259.700	27.766	<b>0.544</b>
	Std.	18.773	5.481	<b>0</b>
200°	Mean	229.155	3.262	<b>0.250</b>
	Best	206.250	2.250	<b>0.250</b>
	Worst	274.000	7.500	<b>0.250</b>
	Std.	13.797	1.294	<b>0</b>
220°	Mean	297.204	7.594	<b>4.246</b>
	Best	245.388	4.666	<b>2.722</b>
	Worst	349.611	19.833	<b>12.833</b>
	Std.	22.486	3.068	<b>1.649</b>
240°	Mean	300.606	4.690	<b>0.333</b>
	Best	239.000	3.000	<b>0.333</b>
	Worst	348.333	10.000	<b>0.333</b>
	Std.	17.747	1.846	<b><math>3.905 \times 10^{-6}</math></b>
250°	Mean	375.483	4.336	<b>0.350</b>
	Best	318.500	3.150	<b>0.350</b>
	Worst	429.100	12.600	<b>0.350</b>
	Std.	20.875	1.519	<b><math>6.694 \times 10^{-16}</math></b>
270°	Mean	255.136	6.121	<b>0.700</b>
	Best	188.650	2.100	<b>0.700</b>
	Worst	322.700	13.650	<b>0.700</b>
	Std.	25.222	3.330	<b><math>1.338 \times 10^{-6}</math></b>

On the other hand, the optimal axial induction factor of the wind turbines in the same row are expected to be the same because the wake propagation is symmetrical as in the case of wind direction at 170°. Eventually, the optimal axial induction factors for each column are represented as  $\{1, 2, 3, 4, 5, 6, 7, 8\} = \{0.2066, 0.1616, 0.1657, 0.166, 0.1728, 0.1160, 0.2640, 0.334\}$ , where the incoming wind speed  $V_\omega$  is directly experienced by the wind turbine in the first row. Noticed that, the axial induction factor of the wind turbines in the last row remains unchanged as the initial axial induction factor. However, the other axial induction factor of the wind turbines in the other rows decreases due to the compensation of the wake effect to the

downstream wind turbines. Consequently, this fact justifies the validity of the proposed grouping strategy, where the convergence time has been significantly improved.

#### 4.4 Performance of Methods with Wind Turbine Failure

In this section, the ability for the MR-ORSSRS, MR-SPSA and ORSSRS based methods to optimize the wind farm in the case of wind turbines failure is presented. Here, the Horns Rev wind farm is simulated to have 5 malfunctioned wind turbines as shown by the circles in Figure 4.12. Meanwhile, the wind is assumed to occur at the direction of  $270^\circ$  with a constant wind speed of  $V_\omega = 8 \text{ m/s}$ , and the algorithm parameters for MR-ORSSRS, MR-SPSA and ORSSRS are set to resemble the case where the wind direction is at  $170^\circ$ , as in the previous section.

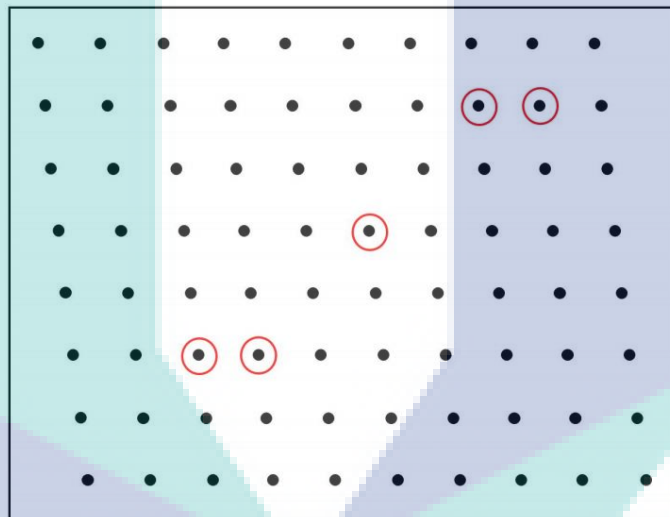


Figure 4.12 Horns Rev wind farm layout with five wind turbine failures.

Figure 4.13 shows the results of the total power production  $\bar{Q}(\alpha_1, \alpha_2, \dots, \alpha_n)$  of MR-ORSSRS, MR-SPSA and ORSSRS based methods for the remaining 75 wind turbines during the first 10 hours of simulation time. The incoming wind is set at  $270^\circ$  with a constant wind speed of  $V_\omega = 8 \text{ m/s}$ . Noticed that the MR-ORSSRS based method converges faster than the MR-SPSA and ORSSRS based methods, as the blue lines are shown to be higher than the green lines and red lines. Meanwhile, Figure 4.14 shows the overall performance of all the methods. All the methods are comparable to obtain the maximum total power production at the 700<sup>th</sup> hour. However, ORSSRS has demonstrated the slowest convergence speed among all three methods.

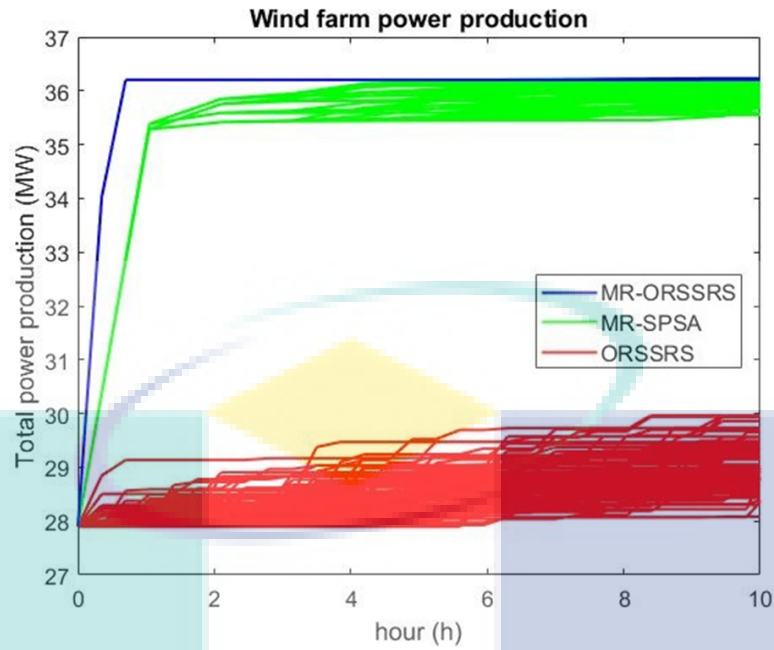


Figure 4.13 Results of the total power production  $\bar{Q}(\alpha_1, \alpha_2, \dots, \alpha_{80})$  during the first 10 hours of simulation time with failure in five wind turbines.

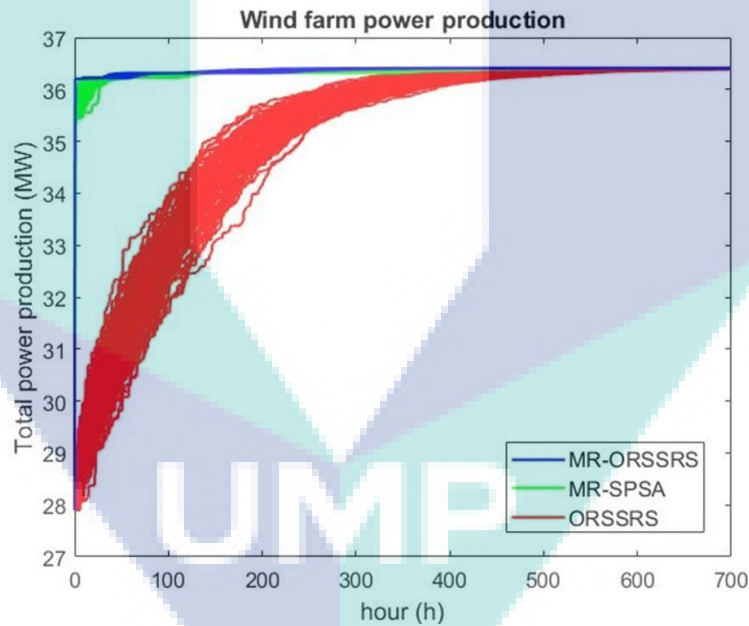


Figure 4.14 Results of the total power production  $\bar{Q}(\alpha_1, \alpha_2, \dots, \alpha_{80})$  of 700 hours of simulation time with failure in five wind turbines.

The statistical analysis of 100 trials is summarized in Table 4.8. Once again, the MR-ORSSRS method outperforms the MR-SPSA and ORSSRS methods to produce the highest total power production in the shortest time. The maximum total power produced by the MR-ORSSRS based method is 36.4142628 MW, while MR-SPSA and ORSSRS based methods merely produce a total power of 36.4139406 MW and 36.4130753 MW. This achievement is yielded by the MR-ORSSRS method within

0.700 hours, while the MR-SPSA and ORSSRS based methods each require 2.100 hours and 186.200 hours to achieve the same result.

Table 4.8 Performance evaluation of the MR-ORSSRS, MR-SPSA and ORSSRS-based methods with five wind turbine failures.

Performance		ORSSRS	MR-SPSA	MR-ORSSRS
Total power production (MW)	Mean	36.4083418	36.4133001	<b>36.4140753</b>
	Best	36.4130753	36.4139406	<b>36.4142628</b>
	worst	36.3863769	36.4115262	<b>36.4135920</b>
	Std. ( $\times 10^{-6}$ )	5135.991	467.422	<b>127.429</b>
Convergence time (h)	Mean	239.246	3.181	<b>0.700</b>
	Best	186.200	2.100	<b>0.700</b>
	worst	285.600	18.900	<b>0.700</b>
	Std.	22.811	2.517	<b><math>1.339 \times 10^{-15}</math></b>

#### 4.5 Performance of methods with non-static Wind Variation

The results presented in previous sections are based on the static wind speed  $V_w = 8 \text{ m/s}$ . However, the fact that the wind condition will vary over time within actual situations should not be overlooked. Therefore, the findings in this section account for the variations in speeds and directions of the incoming wind. Figure 4.15 and Figure 4.16 show the variations of wind speed and direction, respectively, within the duration of 10 hours in simulated time. Here, similar algorithm parameters are applied in MR-ORSSRS, MR-SPSA and ORSSRS from Section 4.3.

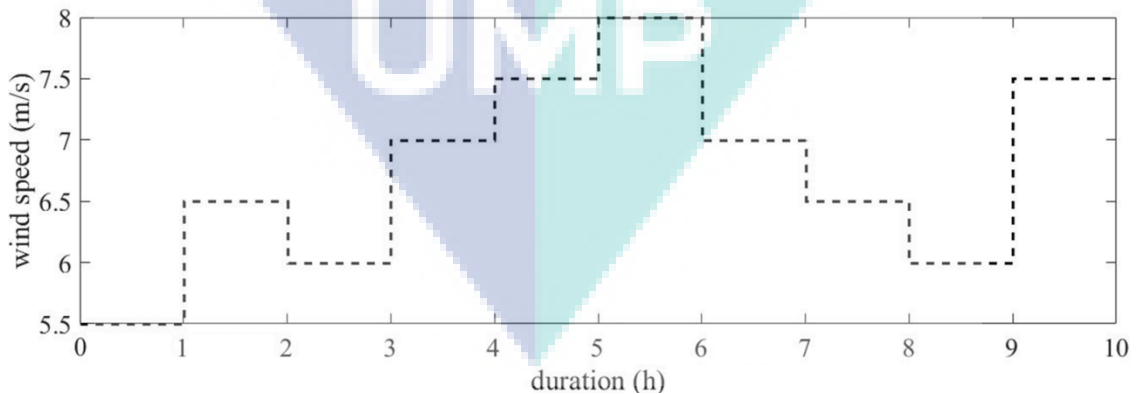


Figure 4.15 Non-Static incoming wind speed variations of 10 hours simulation time.



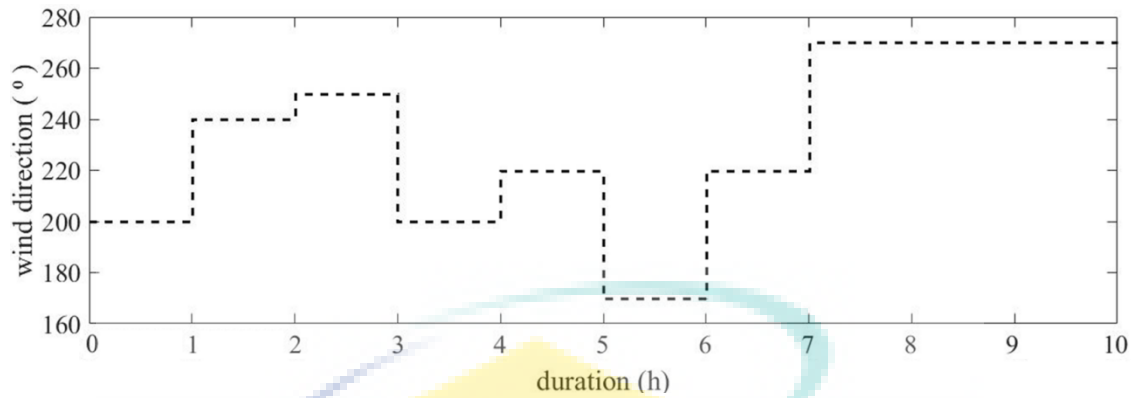


Figure 4.16 Non-Static incoming wind direction variations during 10 hours of simulation time.

Figure 4.17 shows the result of the MR-ORSSRS, MR-SPSA and ORSSRS based methods to improve the total power production  $\bar{Q}(\alpha_1, \alpha_2, \dots, \alpha_n)$  in the case of varying wind speed and direction, in accordance to the patterns shown in Figure 4.15 and Figure 4.16. As evaluated, the MR-ORSSRS based method produces the highest power improvement among the model-free methods when the incoming wind speed and direction vary hourly; yet, with fluctuations in the objective function of this method, in view of the changes in wind condition. Hence, it is understood that the MR-ORSSRS based method will always compute the first resolution of its algorithm during the non-static incoming wind, which further produce responsive power improvements.

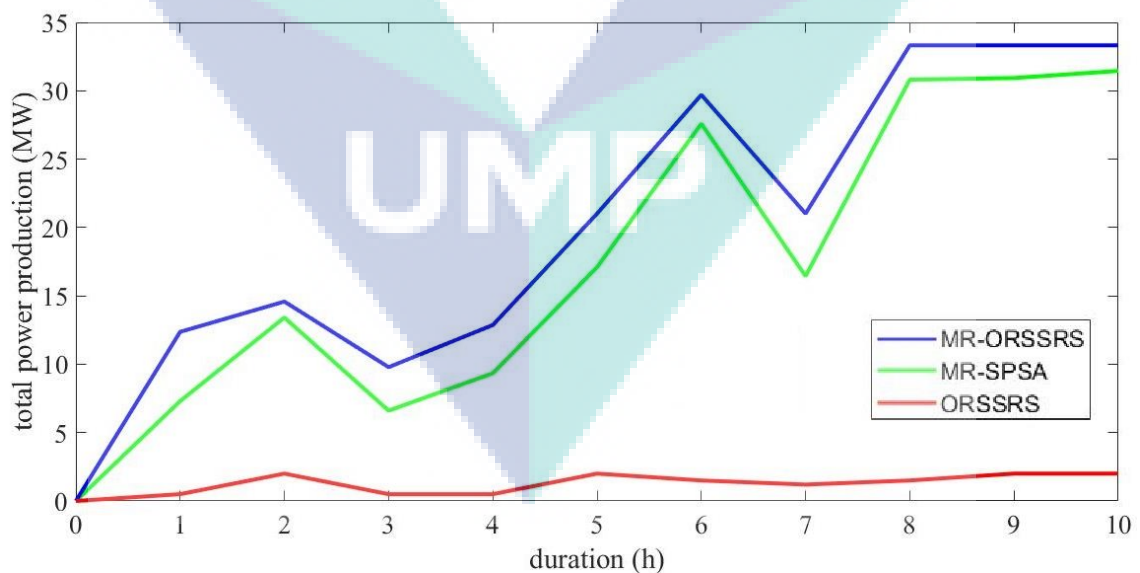


Figure 4.17 Total power improvements of the MR-ORSSRS, MR-SPSA and ORSSRS based methods under non-static incoming wind speed and direction during 10 hours of simulation time.

## 4.6 Summary

In this chapter, the performance of the wind farm's total power production optimization using the MR-ORSSRS, MR-SPSA and ORSSRS based methods have been evaluated. First, the evaluation was conducted according to the static incoming wind, with a constant incoming wind speed of  $V_w = 8 \text{ m/s}$  and wind directions at  $170^\circ, 200^\circ, 220^\circ, 240^\circ, 250^\circ$  and  $270^\circ$ , respectively. Generally, MR-ORSSRS is able to produce the highest total power production with the shortest convergence time, as compared to the MR-SPSA and ORSSRS based methods.

Moreover, the same methods are tested to improve the total power production of a wind farm in the case of wind turbine failure. Five wind turbines are set as failed, where the total power production is produced by the remaining 75 wind turbines in the layout of the Horns Rev wind farm. As expected, the MR-ORSSRS based method remains the option which produces the highest total power production with the shortest convergence time, as compared to the MR-SPSA and ORSSRS based methods.

Lastly, the evaluation of non-static wind speed and direction is provided to validate the performance of real-time application using the new MR-ORSSRS based method. Here, 10 sets of incoming wind speed and direction are simulated within 10 hours of simulation time. Through findings, the performance comparisons show that the MR-ORSSRS based method is responsive to the wind condition, and able to produce the highest total power production in all the variations of incoming wind speed and direction following a real-time manner, overshadowing the performance presented by both the MR-SPSA and ORSSRS methods.

## CHAPTER 5

### CONCLUSION

#### 5.1 Introduction

This chapter outlines the achievements of this research, including its contributions and recommendations for future works. All the objectives of this research have been mentioned in Chapter 1 and have been achieved as a result of the simulations.

In this research, the new Multi-Resolution Optimize Relative Step Size Random Search (MR-ORSSRS) has been used to optimize total power production of a high-dimension wind farm in real-time. Three case studies have been conducted to evaluate the effectiveness and convergence performance of this method, including the incoming wind direction variations, wind turbines failure and non-static incoming wind direction and speed variations. Moreover, another new method known as the standard Optimize Relative Step Size Random Search (ORSSRS) has also been included in this study. The performance of ORSSRS is evaluated based on the same study cases. These two methods have demonstrate their ability in obtaining near optimal solutions for solving high-dimensional wind farm problems. When the simulation results between these two methods are compared, the proposed MR-ORSSRS has improved tremendously from the original ORSSRS, with a higher total power production in a faster convergence speed, in relation to ORSSRS.

Undeniably, the proposed MR-ORSSRS has also proven its superiority against the best results of the other methods reported in recent literature, which include the recently developed MR-SPSA based method. It offers outstanding solutions with the highest total power production and the fastest convergence speed for the three case studies. It demonstrates a stable performance in addressing the six different incoming wind

directions, wind turbines failure and non-static wind speed and direction variations. The proposed MR-ORSSRS based method is shown to perform effectively on a large-scale wind farm, such that of the Horns Rev wind farm which contain 80 wind turbines. Additionally, the proposed method possesses high robustness, and it can minimize fluctuation on the objective function. In this research, it is vital to emphasize that the model-free approach does not require any explicit function of the real-model. This makes it superior in term of simplicity.

Nevertheless, the proposed MR-ORSSRS based method has its weakness. The group strategy must be carefully considered to obtain an optimum optimization performance. This can be seen in Section 3.5 where the group strategy is discussed in detail. Since a group of design parameters of the wind farm problem implement the same solution, it conforms to the characteristics of the MR-ORSSRS based method. In this research, a promising wind farm configuration is implemented in order to fairly analyse the optimized results.

## **5.2 Contribution**

The main contributions of this research towards the advancements in wind farm development are summarized below:

1. A newly developed MR-ORSSRS based optimization algorithm has been implemented to solve the problem in total power production of high-dimensional wind farms. As expected, this method validates its superiority in the ability to produce the highest total power production at the fastest convergence speed, among other rival methods. In the economic point of view, this achievement will further benefit the economic dispatch and secure the operation of the wind farm towards exploiting wind energy for power production. Since MR-ORSSRS has outperformed other options in improving the total power production of high-dimensional wind farms, it might be useful to solve the high-dimensional optimization problems in other fields as well.
2. In term of research objective achievements, the proposed MR-ORSSRS based method has successfully improved the high-dimensional wind farm total power production problem, through its stochastic searching ability, as well as its memorable characteristics for the evaluation of the objective function in every

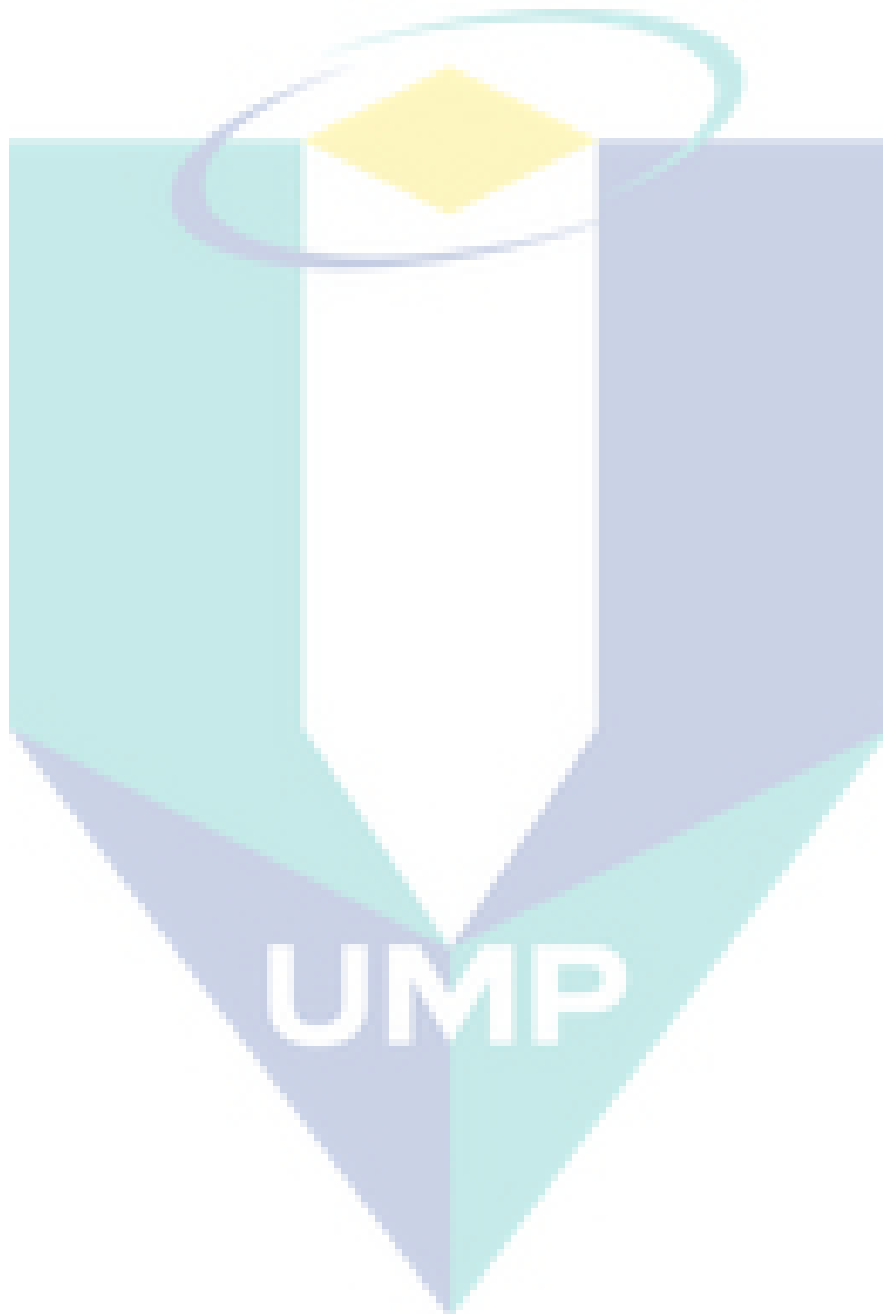
iteration. Additionally, the MR-ORSSRS based method is also able to maximize the total power production of large scale wind farm, up to one consisting of 80 wind turbines, by finding the best combination of the optimal settings of the design parameter. In all the study cases presented, Other methods are demonstrated to be comparatively inferior to the proposed MR-ORSSRS based method, by producing a more optimum performance for both total power production and convergence time. This achievement will be able to assist in solving the critical problems of a high-dimensional wind farm, by reducing the dimension of the design parameter while maintaining the reliability of the total power production.

3. The performance evaluation conducted in this study has fulfilled the equality constrains in the MR-ORSSRS and MR-SPSA based optimization methods. Both the methods have indicated comparable performance in term of total power production. However, the proposed MR-ORSSRS based method can achieve higher stability in total power production as compared to the MR-SPSA. Meanwhile, MR-ORSSRS can achieve faster convergence speed than the existing MR-SPSA based method in all the study cases. In general, the proposed MR-ORSSRS based method has surpassed the existing MR-SPSA based method to consistently produce a higher total power production faster.

### **5.3 Recommendations and Future Works**

This study is mainly focused on the optimization of a wind farm's total power production. Yet, noted that another crucial problem in the wind farm optimization is the fatigue load of the wind turbines in the wind farm, whereby wind turbines which experiences colossal fatigue load will encounter higher potential for damages and breakdowns (Toft *et al.*, 2016). This will subsequently increase the maintenance cost, at the expense of a reduction in productivity of the total power. Nevertheless, minimizing the fatigue load of wind turbines in the wind farm will reduce a wind farm's total power production, further decreases the overall ability for efficient power production. Therefore, a multi-objective optimization of a wind farm for the maximization of the total power production with the minimization of the total fatigue load using MR-ORSSRS based method should be the focus of a future study. This would be an essential field of study,

in maintaining the total power production of the wind farm, while lowering the maintenance cost through minimizing the fatigue load of the wind turbines.



## REFERENCES

- Ahmad, M. A., Azuma, S. I. and Sugie, T. (2014) 'A model-free approach for maximizing power production of wind farm using multi-resolution Simultaneous Perturbation Stochastic Approximation', *Energies*, 7(9), pp. 5624–5646. doi: 10.3390/en7095624.
- Ahmad, M. A., Azuma, S. and Sugie, T. (2014) 'A Model-Free Approach to Wind Farm Control Using Simultaneous Perturbation Stochastic Approximation', pp. 1352–1355. doi: 10.3390/en7095624.
- Bazacliu, G., Lazaroiu, G. C. and Dumbrava, V. (2015) 'Design of wind farm layout for maximum wind energy capture', *UPB Scientific Bulletin, Series C: Electrical Engineering*, 77(1), pp. 269–276. doi: 10.1016/j.renene.2009.08.019.
- Bianchi, F. D., Battista, H. De and Mantz, R. J. (2011) *Wind Turbine Control Systems Principles, Modelling and Gain Scheduling Design, Media*. Available at: <http://www.springer.com/engineering/control/book/978-0-85729-634-4>.
- Chowdhury, S. *et al.* (2012) 'Unrestricted wind farm layout optimization (UWFLO): Investigating key factors influencing the maximum power generation', *Renewable Energy*, 38(1), pp. 16–30. doi: 10.1016/j.renene.2011.06.033.
- Churchfield, M. J. (2013) *Review of Wind Turbine Wake Models and Future Directions (Presentation)*. National Renewable Energy Laboratory (NREL), Golden, CO.
- Ciri, U., Rotea, M. A. and Leonardi, S. (2017) 'Model-free control of wind farms: A comparative study between individual and coordinated extremum seeking', *Renewable Energy*. Pergamon, 113, pp. 1033–1045. doi: 10.1016/j.renene.2017.06.065.
- Dash, P. (2002) 'Automatic generation control of a wind farm with variable speed', *Energy Conversion, IEEE Transactions on*, 17(2), pp. 279–284. doi: 10.1109/TEC.2002.1009481.
- Elkinton, C. N., Manwell, J. F. and McGowan, J. G. (2008) 'Optimizing the layout of offshore wind energy systems', *Marine Technology Society Journal*. Marine Technology Society, 42(2), pp. 19–27.
- Gebraad, P. M. O., van Dam, F. C. and van Wingerden, J. W. (2013) 'A Model-Free Distributed Approach for Wind Plant Control', *2013 American Control Conference (Acc)*, pp. 628–633. doi: 10.1109/ACC.2013.6579907.
- Grady, S. A., Hussaini, M. Y. and Abdullah, M. M. (2005) 'Placement of wind turbines using genetic algorithms', *Renewable Energy*, 30(2), pp. 259–270. doi: 10.1016/j.renene.2004.05.007.
- GWEC (2017) 'Global Wind Report 2016', *Wind energy technology*, p. 76. Available at: <http://files.gwec.net/files/GWR2016.pdf>.

- Hansen, A. D. *et al.* (2006) ‘Centralised power control of wind farm with doubly fed induction generators’, *Renewable Energy*, 31(7), pp. 935–951. doi: 10.1016/j.renene.2005.05.011.
- Herman, S. (2011) *Software assists with wind-farm layouts*, *Windpower Engineering*. Available at: <https://www.windpowerengineering.com/design/software-assists-with-wind-farm-layouts/>.
- Jonkman, J. *et al.* (2009) *Definition of a 5-MW Reference Wind Turbine for Offshore System Development*. National Renewable Energy Laboratory (NREL), Golden, CO. doi: 10.2172/947422.
- Joshua S Hill (2017) *Denmark Generated Enough Wind Energy To Power All Its Electricity Needs On Wednesday*, *Clean Technica*. Available at: <https://cleantechnica.com/2017/02/24/denmark-generated-enough-wind-energy-power-needs-wednesday/>.
- Katic, I., Højstrup, J. and Jensen, N. O. (1986) ‘A simple model for cluster efficiency’, in *European wind energy association conference and exhibition*, pp. 407–410.
- Kristoffersen, J. R. and Christiansen, P. (2003) ‘Horns Rev Offshore Windfarm: Its Main Controller and Remote Control System’, *Wind Engineering*, 27(5), pp. 351–359. doi: 10.1260/030952403322770959.
- Marden, J. R., Ruben, S. D. and Pao, L. Y. (2012) ‘Surveying Game Theoretic Approaches for Wind Farm Optimization’, *50th AIAA Aerospace Sciences Meeting including the New Horizons Forum and Aerospace Exposition*, pp. 1–10. doi: 10.2514/6.2012-1154.
- Marden, J. R., Ruben, S. D. and Pao, L. Y. (2013) ‘A model-free approach to wind farm control using game theoretic methods’, *IEEE Transactions on Control Systems Technology*, 21(4), pp. 1207–1214. doi: 10.1109/TCST.2013.2257780.
- Marmidis, G., Lazarou, S. and Pyrgioti, E. (2008) ‘Optimal placement of wind turbines in a wind park using Monte Carlo simulation’, *Renewable energy*. Elsevier, 33(7), pp. 1455–1460.
- Mohd, A. bin A. (2015) ‘Model-Free Controller Design based on Simultaneous Perturbation Stochastic Approximation’. Kyoto University.
- Mora, J. C. *et al.* (2007) ‘An evolutive algorithm for wind farm optimal design’, *Neurocomputing*. Elsevier, 70(16–18), pp. 2651–2658.
- Mosetti, G., Poloni, C. and Diviacco, B. (1994) ‘Optimization of wind turbine positioning in large windfarms by means of a genetic algorithm’, *Journal of Wind Engineering and Industrial Aerodynamics*, 51(1), pp. 105–116. doi: 10.1016/0167-6105(94)90080-9.



- Mustakerov, I. and Borissova, D. (2010) 'Wind turbines type and number choice using combinatorial optimization', *Renewable Energy*. Elsevier, 35(9), pp. 1887–1894.
- Nielsen, P. (no date) 'EMD international A', *S, WindPRO*, 2, pp. 179–181.
- Park, J., Kwon, S. and Law, K. H. (2013) 'Wind farm power maximization based on a cooperative static game approach', *SPIE Smart Structures/NDE Conference*, 8688, pp. 1–15. doi: 10.1117/12.2009618.
- Park, J. and Law, K. H. (2016) 'A data-driven, cooperative wind farm control to maximize the total power production', *Applied Energy*, 165, pp. 151–165. doi: 10.1016/j.apenergy.2015.11.064.
- Park, J. and Law, K. H. (2016) 'Bayesian Ascent: A Data-Driven Optimization Scheme for Real-Time Control With Application to Wind Farm Power Maximization', *IEEE Transactions on Control Systems Technology*, 24(5), pp. 1655–1668. doi: 10.1109/TCST.2015.2508007.
- Porté-Agel, F., Wu, Y.-T. and Chen, C.-H. (2013) 'A Numerical Study of the Effects of Wind Direction on Turbine Wakes and Power Losses in a Large Wind Farm', *Energies*, 6(10), pp. 5297–5313. doi: 10.3390/en6105297.
- Scholbrock, A. K. (2011) 'Optimizing Wind Farm Control Strategies to Minimize Wake Loss Effects'.
- Schumer, M. A. and Steiglitz, K. (1968) 'Adaptive Step Size Random Search', *IEEE Transactions on Automatic Control*, 13(3), pp. 270–276. doi: 10.1109/TAC.1968.1098903.
- Serrano Gonzalez, J. *et al.* (2014) 'A review and recent developments in the optimal wind-turbine micro-siting problem', *Renewable and Sustainable Energy Reviews*, pp. 133–144. doi: 10.1016/j.rser.2013.09.027.
- Şişbot, S. *et al.* (2010) 'Optimal positioning of wind turbines on Gökçeada using multi-objective genetic algorithm', *Wind Energy*. Wiley Online Library, 13(4), pp. 297–306.
- Soleimanzadeh, M. and Wisniewski, R. (2011) 'Controller design for a wind farm, considering both power and load aspects', *Mechatronics*, 21(4), pp. 720–727. doi: 10.1016/j.mechatronics.2011.02.008.
- Soleimanzadeh, M., Wisniewski, R. and Kanev, S. (2012) 'An optimization framework for load and power distribution in wind farms', *Journal of Wind Engineering and Industrial Aerodynamics*, pp. 256–262. doi: 10.1016/j.jweia.2012.04.024.
- Spall, J. C., Hill, S. D. and Stark, D. R. (1999) 'Theoretical comparisons of evolutionary computation and other optimization approaches', in *Proceedings of the 1999 Congress on Evolutionary Computation, CEC 1999*, pp. 1398–1405. doi: 10.1109/CEC.1999.782646.

- Spudic, V. (2010) 'Hierarchical wind farm control for power/load optimization', *The Science of making Torque from Wind (Torque2010)*, pp. 1–3.
- Spudic, V., Jelavic, M. and Baotic, M. (2011) 'Wind Turbine Power References in Coordinated Control of Wind Farms', pp. 82–94.
- Sveinbjornsson, S. K. (2013) 'Analysis of WAsP (Wind Atlas Analysis and Application Program) in complex topographical conditions using measured production from a large scale wind farm.'
- Toft, H. S. *et al.* (2016) 'Uncertainty in wind climate parameters and their influence on wind turbine fatigue loads', *Renewable Energy*. Elsevier, 90, pp. 352–361.
- Truepower, A. W. S. (2010) 'OPENWIND Theoretical Basis and Validation', *Albany, NY, Technical Report*, (1.3).
- Vincent, S. (2009) *GH WindFarmer theory manual*.
- Wan, C. *et al.* (2012) 'Wind farm micro-siting by Gaussian particle swarm optimization with local search strategy', *Renewable Energy*. Elsevier, 48, pp. 276–286.
- Yin, P.-Y., Wu, T.-H. and Hsu, P.-Y. (2017) 'Risk management of wind farm micro-siting using an enhanced genetic algorithm with simulation optimization', *Renewable Energy*, 107, pp. 508–521. doi: 10.1016/j.renene.2017.02.036.

The logo for UMP (University of Management and Pedagogy) is a large, stylized shield shape. It is composed of several overlapping geometric shapes in shades of teal, light blue, and yellow. The letters 'UMP' are prominently displayed in white, bold, sans-serif font across the bottom center of the shield.

UMP

## LIST OF PUBLICATION

1. M.A. Ahmad, M. Ren Hao, R.M.T. Raja Ismail, A.N.K. Nasir, "Model-free wind farm control based on random search", Proceedings of IEEE International Conference on Automatic Control and Intelligent Systems, 2016, pp. 131-134.
2. M.R. Hao, R.M.T. Raja Ismail, M.A. Ahmad, "Using spiral dynamic algorithm for maximizing power production of wind farm", Proceedings of IEEE International Conference on Applied System Innovation, 2017, pp. 1706-1709.
3. M.R. Hao, M.A. Ahmad, R.M.T. Raja Ismail, A.N.K. Nasir, "Performance evaluation of random search based methods on model-free wind farm control", Lecture Notes in Mechanical Engineering, 2018, pp. 657-670. ISBN 978-981-10-8787-5.
4. M.R. Hao, R.M.T. Raja Ismail, M.A. Ahmad, "Model-free wind farm control based on multi-resolution optimized relative step size random search", Applied Soft Computing, ISI index (will be submitted)



UMP